Control Aspects of the Brushless Doubly-Fed Machine

Bonneville
POWER ADMINISTRATION

September 1990

CONTROL ASPECTS OF THE BRUSHLESS DOUBLY-FED MACHINE

DOE/BP/24332--1

DE91 009707

Contract No. 79-85BP24332, MOD-6

FINAL REPORT
September 1990

By : Hian K. Lauw and Sheela Krishnan
Oregon State University
Department of Electrical and Computer Engr.
Corvallis, OR 97331 Tel : (503)737-3617

DISCLAIMER

Prepared for

U.S. DEPARTMENT OF ENERGY
BONNEVILLE POWER ADMINISTRATION
PORTLAND, OREGON 97208

TABLE OF CONTENTS

LIST OF FIGURES

ACKNOWLEDGEMENTS

The authors wish to thank Mr. Walt Myers and Mr. Nicholas Butler from the Bonneville Power Administration for their confidence in us to carry out this work. In particular, we greatly appreciate Mr. Butler's efforts in facilitating the progress of our research, along with his useful suggestions to enhance the quality of this final report.

We also wish to express our gratitude to Mr. Claus Weigand for trouble-shooting the series-resonant converter during the few occasions that the design limits of the converter were violated while testing the operating capabilities of the variable-speed generation system. Mr. Ashok Ramchandran's efforts and advice in interfacing the converter with the controller for variable-speed operation as well as the required signal processing tasks, were extremely valuable.

1. ABSTRACT

This report covers the investigations into the control aspects of a variable-speed generation (VSG) system using a brushless doubly-fed generator excited by a series-resonant converter. The brushless doubly-fed machine comprises two sets of stator 3-phase systems which are designed with common windings. The rotor is a cage rotor resembling the low-cost and robust squirrel cage of a conventional induction machine. The system was actually designed and set up in the Energy Laboratory of the Department of Electrical and Computer Engineering at Oregon State University. The series-resonant converter designed to achieve effective control for variable-speed generation with the brushless doubly-fed generator was adequate in terms of required time response and regulation as well as in providing for adequate power quality. The three elements of the VSG controller, i.e. voltage or reactive power controller, the efficiency maximizer and the stabilizer, could be designed using conventional microprocessor elements with a processing time well within the time period required for sampling the variables involved with executing the control tasks. The report treats in detail the stability problem encountered in running the machine at certain speed regions, even if requirements for steady-state stability are satisfied. In this unstable region, shut down of the VSG system is necessary unless proper stabilization controls are provided for. The associated measures to be taken are presented.

2. INTRODUCTION

This report covers work on the sixth extension (Mod-6) to the research contract No. 79-BP24332 which was awarded by the Bonneville Power Administration (BPA) to Oregon State University (OSU) on October 31, 1988.

The work involved with the earlier extensions (Mod-1, Mod-2, and Mod-3) covered investigations into the characteristics of a Variable-Speed Generation (VSG) system, followed by an actual design of a 15 kW unit in the laboratory (see Ref.1 through 4). In this system, a doubly-fed generator is used with the rotor windings excited through slip-rings by a series-resonant converter. The system has been demonstrated to be capable of :

- operating at a wide shaft-speed range (including zero RPM as well as positive and negative values) by simply controlling the output frequency of the converter,
- operating with maximum efficiency at any speed,
- generating or absorbing reactive power,
- controlling the frequency and magnitude of the stator voltage for stand-alone operation.
- providing generator voltage and current waveforms satisfying standards specified by the proposed IEEE/ANSI-519 standard.

A cost benefit analysis was also reported on, indicating that the VSG system is a viable alternative to the conventional fixed-speed generation systems if sufficient fluctuations prevail in the primary energy resource (Ref.1).

Since the air-gap of the doubly-fed generator is not required to be as narrow as that of an induction machine, doubly-fed generators can be used for VSG systems rated at hundreds of MW. For VSG systems rated at 10 MW or less, the brushless doubly-fed generator is an attractive alternative in that no slip-rings or brushes are needed and a low-cost, robust rotor

similar to the cage rotor of an induction machine can be used.

The subject of investigations in the fourth extension of the agreement (Mod-4) was indeed regarding the characteristics of the brushless doubly-fed machine as invented by Hunt in 1907 (Ref.5) and its viability for a VSG system (Note: Mod-5 only covered an administrative matter). A 1 HP machine was designed for this purpose, followed by a 15 HP version after the proof of Hunt's concept was found to be satisfactory. The required two sets of 3-phase systems were built with common windings. Results of the study during the course of the fourth extension were documented in Ref.6 which includes a convenient tool of analysis to understand the performance of the machine in the synchronous mode. The investigations revealed that the brushless doubly-fed machine can be operated in either the induction mode or synchronous mode. The synchronous mode was found to result in a higher efficiency and obviously has the advantage of providing shaft-speed control without the need for a speed signal feedback. Moreover, in the synchronous mode reactive power (and hence power factor) and the shaft-speed can be independently controlled.

A requirement for operating the brushless doubly-fed machine in the synchronous mode at any speed is the availability of a power electronic converter capable of:

- regenerative operation and smooth transition from AC to DC as well as smooth phase sequence reversal.
- operating in the step-up mode, i.e. transferring power from the low-voltage side to the high-voltage side of the converter.
- providing voltage and current output waveforms satisfying voltage and current harmonic requirements specified by the proposed IEEE/ANSI-519 standard.
- not absorbing excessive reactive power from the electric grid to which the input side is connected, irrespective of the shaft-speed (in order to facilitate unity power factor operation of the doubly-fed machine).

Regenerative operation of the converter is needed if: (1) the machine runs as a motor below the synchronous speed, and (2) the machine runs as a generator above the synchronous

speed. Moreover, in this case power needs to be transferred from the low- to the high-voltage side of the converter. The voltage is extremely low (compared to the high-voltage side) if the machine runs near synchronous speed. The use of a series-resonant converter has been demonstrated to meet these requirements satisfactorily, including frequency separation between the two sets of 3-phase stator systems.

The following tasks were included to the Statement of Work for this sixth extension of the research contract:

- Task (15): Set up complete laboratory-scale VSG system using a brushless doubly-fed generator and a series-resonant converter.
- Task (16): Design and implement an integrated system controller, including the efficiency maximizer, voltage and reactive power controller, and supervisory control logic.
- Task (17): Documentation and demonstration of designed VSG system performance.

The execution of all of these research activities has turned out to be premature due to the discovery of dynamic stability problems during the course of this research. In Ref.6 where the theory of the machine's performance was presented, the existence of steady-state stability limits was predicted. This work gave evidence that the current of the 3-phase system with the lower number of pole-pairs is required to be bounded between lower and upper limits dependent on the amount of shaft power. This theory was confirmed with experiments conducted on the designed machine. However, the dynamic stability problems could not be predicted through the use of a steady-state model. The observed dynamic instability in certain speed regions were considered to be due to inadequate shaft-centering or resonance associated with the inertia system associated with the electromechanical energy conversion process. Moreover, since this instability only occurs in a relatively small speed region, at the time other priorities in the research were pursued.

During the course of conducting the work for this sixth extension, it was conclusively determined that the instability problem encountered is not due to the violation of the

predicted steady-state limits, but is rather due to a phenomenon associated with dynamic stability. We became more convinced after a literature search pointed us to a paper by Cook and Smith (Ref.7) where the existence of such a dynamic instability region was reported with their computer study of a system consisting of 2 induction machines with a common rotor. Such a system could be considered a simplified version of the brushless doubly-fed machine. It is reasonable to expect that certain essential performance features of the system studied by Cook and Smith would apply as well to those of the brushless doubly-fed machine, even though the brushless doubly-fed machine is designed with a single stator containing common windings for two sets of 3-phase stator windings .

It was mentioned before that instability occurs in a relatively small speed region. Nevertheless, careful observations of this dynamic instability phenomenon have led to the conclusion that continuous operation of the VSG system with the brushless doubly-fed machine is at such a risk, that acceptance of the machine for a VSG application should be rejected unless this dynamic instability problem could be contained. It was felt, therefore, that all efforts have to be devoted to the design of a stabilizer for the designed doubly-fed machine. Only if these efforts are successful, would it be worthwhile pursuing the original tasks as reflected in the Statement of Work.

Documentation of the design of the stabilizer and the evaluation of its effectiveness are provided in this final report. It is shown that only partial success could be established in the sense that, even though the stabilizer is capable of preventing a loss of synchronism in the unstable speed region, that bounded oscillations of the shaft-speed in this region can not be prevented. Moreover, the steady-state stability limits which would be acceptable in the absence of the dynamic stability problem, are significantly reduced in the dynamic unstable region. An approach which could force the system to obtain extra damping in a non-dissipative way at the expense of including a shaft-speed signal feedback in the stabilizing control logic, will be presented.

However, in a later stage of the research, it became apparent that complete success of

the brushless doubly-fed machine using common windings for the two sets of stator 3-phase systems is basically doubtful. The design requires these two sets to have common windings and yet to have differing number of poles. The resulting need for a compromise in the design which would lead to undesirable effects on the dynamic stability, will be explained. There is a need to resolve this problem with a different design. Documentation on this continuing work for a different research contract will not be included in this final report.

It is remarked in closing this introduction that even though the effectiveness of the designed stabilizer for the brushless doubly-fed machine using common windings for the two sets of 3-phase stator systems was found to be marginal, the use of this stabilizer for a machine with a different design may still be needed to improve its transient characteristics. This could for instance be the case if a fast change of the shaft-speed is desired or if the load torque (or prime mover in case of a generator) is experiencing large fluctuations in magnitude. The effectiveness of the stabilizer was observed for a VSG system driven by an automotive engine on another research project. This VSG system was equipped with the conventional doubly-fed machine (requiring brushes and slip-rings) as considered in the study for the earlier extensions of the contract (Ref.1 through 4). This system was demonstrated to have superior stability characteristics and did not suffer from dynamic stability problems under reasonably normal conditions. Yet, the severe automotive engine torque pulsations with every revolution (ranging from negative to positive values) cause the doubly-fed machine (during fast engine speed run-ups) to lose its synchronism if no stabilizer is provided.

3. MAJOR COMPONENTS OF VSG SYSTEM

The variable-speed generation (VSG) system using a brushless doubly-fed machine was readily tested in the Energy Laboratory of the Department of Electrical and Computer Engineering at Oregon State University. Much of the equipment and needed measurement instruments were acquired during the course of the second extension (Mod-2) to the research contract (Ref.3).

For convenience to the reader, the structure of the VSG system as set up in the laboratory will be reintroduced along with the description of modifications to this structure and the brushless doubly-fed machine, replacing the conventional doubly-fed machine which was subject to study and documentation in Ref.3. This chapter will be restricted to coverage of the hardware components of the VSG system. Discussion on the VSG controller using the brushless doubly-fed generator will be presented the next chapter.

3.1 SYSTEM CONFIGURATION

In Fig.3.1 the VSG system (about 15 HP in rating) as set up in the Energy Laboratory is shown. Two machine-sets can be observed. The machine set in front is the brushless doubly-fed machine (on the right) driven by a DC motor (on the left). A torque transducer is visible on the shaft system which couples the doubly-fed machine and the DC motor. The machine-set in the back consists of a conventional doubly-fed machine (rotor winding with slip rings and brushes) driven by a DC motor. Both DC motors are under control of a four-quadrant AC-to-DC converter which makes it possible to study and test the machine performance for different power-speed characteristics depending on the particular energy resource dealt with. Two boxes are shown behind the machine sets; the box on the right is the series-resonant converter and the one on the left the mentioned AC-to-DC converter to control the DC motors.

A VSG system can be viewed to consist of five major components: the brushless doubly-fed generator, the power electronic converter, the turbine, the electric power grid and the VSG controller needed to assure proper operating conditions. Fig. 3.2 shows the schematic block diagram of this system. It is to be noted that the stator of the brushless doubly-fed machine contains two sets of 3-phase systems. The number of poles of these systems is different and for the designed machine are chosen to be 2 and 6 poles. The output of the converter is to be connected to the 3-phase system with the lower number of poles, i.e. the 2-pole system. The input of the converter is connected to the same three-phase electric power grid to which the 6-pole, 3-phase system is connected. The block diagram shows the hardware components of the VSG system as well as the various subcontrollers of the VSG controller with their required sensors and connections of output signals.

The choice of the shown topology for the VSG system reflects a desire to achieve a VSG system which is a viable alternative to the conventional fixed-speed generation system (FSG) in terms of cost with improved efficiency, flexibility and performance. The bulk of the additional cost of a VSG system as compared to a conventional FSG system is due to the cost of the power electronic converter. The cost benefit of the proposed VSG system stems from the fact that the power electronic converter in the chosen topology is only required to process a fraction of the total mechanical power to be converted into electric power. This fraction is equal to about the ratio of the number of pole-pairs of the two sets of stator 3-phase systems, which for the designed machine corresponds with one third (see Ref.6). Economic viability of this VSG system for hydro or wind energy applications is expected to be determined by the same factors as discussed in Ref.1 which basically require sufficient fluctuations in the primary energy resource such that it is possible to assure a significant energy gain as compared to the electric energy generated by a fixed-speed generation system. For economic viability in other generation applications such as peak power shaving and intermittent power buffering, the energy gain requirement is not crucial. In these systems, the capability of the VSG system to generate additional power for limited periods of the day provides the economic incentive. This is due the capability of a VSG to increase the shaft-speed beyond the synchronous speed of an FSG system.

Another important reason for the choice of the proposed VSG system topology is the possibility to achieve functional capabilities which at least preserve those which can be obtained from a conventional FSG system. This includes reactive power generation control (thus power factor control) and/or voltage control, as well as the obvious capability of a VSG system to control the shaft-speed electronically for continuous maximum-efficiency over the full operating range.

3.2 BRUSHLESS DOUBLY-FED GENERATOR

Fig.3.3 is a close-up of the brushless doubly-fed machine shown as item No. 5 in Fig. 3.1. The brushless doubly-fed machine (to the right of the torque transducer) has a housing for a forced air cooling system. This forced cooling is to facilitate study of the system at low shaft speeds when the airflow through the air gap is practically non-existent.

The design aspects, and an actual design exercise, of the brushless doubly-fed machine using common windings for the two sets of 3-phase stator systems were documented in detail in Ref.6. Fig.3.4 shows the corresponding wiring diagrams. The resulting machine which was used during the course of this contract has the following rating and parameters:

- 15 HP, 120 V, 1200 RPM,
- Stator: 36 slots with the 2- and 6-pole 3-phase stator systems using common windings; pole pitch spanning slot numbers 1 and 10; 60 turns for each coil; wire size 19 (American wire gauge, i.e. 1288 cmills),
- Rotor: 36-slot squirrel cage with 4 squirrel-cage bars in slot numbers 1, 10, 19 and 28; 4 short-circuited bars between any two squirrel-cage bars,
- Single-phase equivalent machine parameters (see Ref.6 for diagram):

  R_1 = 1.13 Ohm = stator resistance of 6-pole system

  X_1 = 2.18 Ohm = leakage reactance of 6-pole system (at 60 Hz)

  R_2 = 1.13 Ohm = leakage resistance of 2-pole system

  X_2 = 1.44 Ohm = leakage reactance of 2-pole system (at 60 Hz)

R_r = 2.63 Ohm = total rotor resistance

X_{m1} = 33.51 Ohm = main reactance of 6-pole system (at 60 Hz)

X_{m2} = 22.15 Ohm = main reactance of 2-pole system (at 60 Hz)

The premise of the chosen control strategy which will be discussed in the next chapter depends on the way the brushless doubly-fed machine is operated. For the reader's convenience, a review of the possible modes of operation of the brushless doubly-fed machine which was investigated in a previous extension to the research contract and documented in Ref.6, will be presented. The section will be concluded with the preferred mode of operation to which the VSG control strategy will be tailored.

The machine can be either operated in the singly-fed or doubly-fed mode. In the singly-fed mode, the first of the two sets of stator 3-phase systems is connected to a frequency source which is always the electric utility grid. The second stator 3-phase system is connected either to a passive network or a DC-link converter with the rectifier side connected to the machine. In this case, the machine operates exclusively in the induction mode as can be explained as follows. Dependent on the RPM, the current with frequency f_{s1} (60 Hz if connected to US electric grid) in the first stator 3-phase system induces a rotor current of a certain frequency f_r which in turn induces a current with a frequency f_{s2} in the second stator 3-phase system. Therefore, the frequency f_{s2} is by virtue of the induction phenomenon and is not a supply frequency. This frequency is determined by the ambient RPM which depends on how the machine's torque-speed characteristic is matched to the torque-speed characteristics of the mechanical load or prime mover.

In the doubly-fed mode, the two sets of stator 3-phase systems are connected to independent frequency sources, i.e. f_{s1} and f_{s2} are both truly supply frequencies. The first set of 3-phase stator systems (with the higher number of poles) is connected to the electric power grid which in the US provides a supply frequency of 60 Hz. The second set of stator 3-phase systems with the lower number of poles is connected to a power electronic converter capable of supplying output current waveforms with controllable frequency f_{s2}. As opposed

to the singly-fed mode, the doubly-fed mode provides the possibility to operate in both the induction mode and synchronous mode. However, it was explained in Ref.6 that the doubly-fed induction mode should be used only during short overload of if synchronism is temporarily lost since the associated efficiency is significantly lower than that of the doubly-fed synchronous mode.

The VSG system controller, to be covered in the next chapter, is proposed to be designed on the premise that the brushless doubly-fed generator is operated in the doubly-fed synchronous mode (rather than the singly-fed mode) for the following reasons:

(a) In the singly-fed mode, the machine is only capable of running like a conventional induction machine and, therefore, is not capable of generating reactive power.

(b) The shaft-speed in the proposed doubly-fed synchronous mode of operation is dictated by the supply frequencies of the two sets of stator 3-phase systems. Therefore, shaft-speed control is merely a matter of providing the associated reference signal for the output frequency of the converter to obtain the variable supply frequency of the second stator 3-phase system (with a lower number of poles). The supply frequency for the first stator 3-phase system is obtained from the electric power grid (60 Hz in the US).
Since the machine operates in the synchronous mode, the resulting RPM will have a tight variation margin without the need to supply a speed sensor feedback signal to the VSG controller.

(c) Shaft-speed control and reactive power (thus also power factor) control are decoupled, i.e. shaft-speed and reactive power are independent in the doubly-fed synchronous mode. Reactive power can be varied by simply varying the output current amplitude of the converter, whereas the shaft speed as mentioned above, can be changed by varying the output frequency of the converter.

(d) Reactive power generation is possible in the doubly-fed synchronous mode, provided that a power electronic converter (like the series-resonant converter) is used which at the input side would not demand for excessive reactive power from the electric grid to which the converter is connected.

3.3 SERIES-RESONANT CONVERTER

The function of the series-resonant converter (SRC) is to provide excitation power and a means of controlling the brushless doubly-fed machine. Fig. 3.6 is a close-up of the SRC also shown in the picture of the entire VSG system in Fig. 3.1. This converter is an updated version of the one used during the course of the investigations reported in Ref.3. The converter is not a commercial unit and was built entirely in the laboratory. The converter rating is 15 kVA / 230 V / 20 kHz modulation. Success of the SRC in meeting the specific requirements of a VSG system as well as providing adequate output waveforms (satisfying the proposed IEEE/ANSI-519 standard) was discussed in the INTRODUCTION of this report and was documented in detail in Ref.2 and 4. Moreover, this converter was considered ideal in conducting investigative experiments with the control of the brushless doubly-fed machine due to the converter's flexibility to be used either as a programmable voltage or current source. To aid the discussion on the VSG controller in the next chapter, a brief description of the main features of the SRC will be repeated in this report for convenience of the reader (a more detailed description can be found in Ref.2). This description will also include the significance of these features to the operation of the VSG system.

3.3.1 Power Circuit :

The upper part of Fig. 3.6 shows the basic topology of a 3-phase AC-to-AC SRC. The converter consists of an input (SM_a) and an output (SM_b) switching matrix which are

connected to each other with a resonant circuit (L_r, C_r). The resonant circuit is in the direct energy path and serves as a high-frequency AC link. The switching matrices are configured as full-wave bridges. A half-bridge version with half the number of semiconductors is possible (patent pending, by Klaassen, Lauw and De Beer).

3.3.2 Converter Controls:

The lower part of Fig.3.6 shows the schematic of the main converter controls in an abstract sense. The control logic can be observed to be built up by two sections: a high-frequency section which makes decisions on a pulse-by-pulse basis, and a low-frequency section which facilitates feedback signal processing dependent on the application dealt with, such as constant voltage over frequency ratio or vector control. The qualifications of high and low frequency are relative to the frequency of the internal waveform (resonant current) which is significantly higher than the frequency of the input and output waveform. Typically the internal frequency is in the order of 20 kHz and the input and output waveforms are 60 Hz or lower (depending upon the application of the converter).
Fig.3.6 shows that the high-frequency section consists of 3 subcontrollers:

- ASDTIC, the Analog Signal to Discrete Time Interval Converter, which coordinates the semiconductor firing schedule to excite the resonant circuit of the SRC such that a high-frequency carrier is generated. This carrier is subjected to a modulation process which causes the carrier to contain the frequency content of the desired lower frequency spectrum of the output waveforms. The modulation process used is pulse-area modulation, which basically determines the initiation of subsequent resonant-current cycles on the basis of equal area (integral) under the reference signal and the resonant current pulse (as function of time).

- PCL, the peak current limiter which contains a predictor to control the peak value of the resonant current dependent on the load conditions under regular as well as

irregular conditions. The PCL prevents the SRC from requiring excessive peak currents and tailors the peak value depending on the demand by the load, in order to maintain a flat efficiency curve for partial load conditions.

- Resonant Current Distributor contains the logic for choosing the current path for the resonant current to the input and output phases. This logic basically causes adequate time-sharing of the single resonant circuit by all of the input and output phases. Time sharing is possible due to the relatively high resonant frequency as compared to typical frequencies of input and output waveforms.

3.3.3 Filtering Requirements:

One of the undesirable side effects of a VSG system using a power electronic converter as a control means is the harmonic distortion of voltage and current waveforms generated by the converter, and therefore, by the VSG system. The proposed IEEE/ANSI-519 standard requires generators to have a maximum of 5% THD (total harmonic distortion) for the current and a maximum notch depth on the line-to-line voltage of 20% (for general systems). Many proposed VSG systems use a kind of converter known as the cycloconverter mainly because of its capability for continuous and smooth transition from AC to DC which is needed during operation near synchronous speed. However, this kind of a converter was reported to cause a THD of 140%, which, with special harmonic cancellation efforts, is speculated to be reducable to 70% (Ref. 9). Nevertheless, even such an "improved" system is not acceptable to the utility industry unless additional harmonic filters are installed. These filters are not only bulky and expensive, but require adaptive filtering strategies due to the varying frequency spectrum.

The purpose of applying a control strategy based on modulation (high-frequency switching) is to dispense with the need for obtaining the desired accuracy of the output waveform (such as meeting the proposed IEEE/ANSI-519 standard) through bulky and

expensive passive filters. The high-frequency carrier of the SRC is prevented from penetrating the source and the load by a low-pass filter to filter out the high-frequency content of the carrier (20 kHz). Such a filter obviously does not compromise the desired converter's speed of response.

3.3.4 Efficiency:

The accuracy of the output waveform is obviously proportional to the switching frequency. On the other hand, the higher the switching frequency, the higher the switching losses, and therefore, the lower the efficiency. Particularly with forced commutated switching schemes, the switching frequency is limited by the desire to maintain an acceptable level of efficiency.

With the SRC, this problem is mitigated by the resonant circuit in the AC link which makes it possible to apply a soft-switching firing scheme, i.e natural commutation (zero-current and/or zero-voltage switching) of all semiconductors. The SRC is capable of accomplishing an efficiency in the 95%-plus region, in spite of the use of low-cost thyristors (as compared to Mosfets or IGBT's) and a converter modulation frequency of 20 kHz.

3.3.5 Step-down and Step-up:

The input side of a converter is usually connected to the electric utility and the output to a load. The line-to-line voltage at the input terminals of the converter may be higher or lower than that at the output terminals. Certain kinds of converters are only capable of transferring average energy from the high-voltage side to the low-voltage side of the converter. In this case the converter is said to transfer energy in the step-down mode. The step-up mode requires the converter to be capable of transferring average energy from the low-voltage side to the high-voltage side.

A VSG system requires the use of a converter capable of operating in both the step-down and step-up modes. If the system operates near synchronous speed , the terminal voltage of the brushless doubly-fed machine stator 3-phase system connected to the converter is rather low. The other (higher voltage) side of the converter is connected to the electric utility grid. Therefore, as the shaft-speed is controlled to be higher than the synchronous speed, energy needs to be transferred through the converter in the step-up mode. The brushless doubly-fed machine running as a motor, requires the step-up mode for speeds lower than the synchronous speed.

The SRC inherently facilitates both the step-down and step-up modes of operation and logic is provided which automatically detects and executes either of these mode. A detailed explanation can be found in Ref.8. Heuristically, the resonant capacitor can be viewed as a reservoir of energy, and energy can be stored or retrieved by either side of the converter irrespective of the voltage level. This degree of freedom is basically exploited in the semiconductor firing strategy to transfer average energy in either direction, irrespective of the voltage levels at the input and output terminals of the SRC.

3.3.6 AC and DC Output:

The VSG system using a brushless doubly-fed machine requires the use of a converter capable of providing both AC and DC output waveforms and continuous transition from AC to DC and vice versa. The SRC basically does not distinguish between DC or AC input and output waveforms, i.e. the control strategy of the converter is the same for AC or DC. This is due to to the high value of the carrier frequency and the inherent capability of the SRC to operate in the step-down as well as step-up mode (see Ref.2). An output frequency of 60 Hz can be considered as a slowly varying DC signal compared to the carrier signal with a frequency of 20 kHz.

3.3.7 Output Characteristics:

The SRC is inherently bidirectional, i.e. four-quadrant AC and DC output characteristics are possible. The SRC was described as capable of operating as a voltage source or a current source. Amplitude and frequency are controllable in both modes with negligible time-constants (compared to the machine time-constants). It was mentioned in Ref.2 that the conventional doubly-fed machine (having brushes and slip rings for the rotor windings) benefits from the use of current-source converter. Negative damping torques would be possible in certain speed regions if a voltage-source converter is used. The brushless doubly-fed machine seems to be insensitive to operation with either a current-source or voltage-source converter. However, since it is the current which governs the performance of any electric machine, the use of a current-source converter provides a more direct means of control.

3.4 TURBINE

The hydro turbine characteristics under varying pressure head and gate position were discussed in Ref.1 in which it was shown that the power-speed characteristics assume a cubic relationship if the turbine is operated at maximum efficiency. These characteristics also apply to wind turbines if the gate position parameter is replaced with the pitch angle and the pressure head replaced with wind speed. For fixed-pitch wind turbines, the pitch angle parameter would not be needed.

The turbine is simulated in the laboratory VSG system by a separately excited DC motor drive under control of a regenerative Reliance DC-to-DC converter. This provides the flexibility to control the field voltage as well as the armature voltage of the DC motor. These voltages can be manually adjusted to study, for instance, the performance of the brushless doubly-fed machine at maximum-torque conditions. Reference signals for these voltages are also accepted and processed in a feedback control logic which makes it possible

to program any power-speed characteristic of the DC motor for driving the brushless doubly-fed machine, functioning as the generator of the VSG system.

Measurements were conducted to find the correlation between the armature voltage and the motor speed to achieve the cubic power-speed curve corresponding to maximum-efficiency operating conditions of an actual turbine. These measurements provide a curve reflecting the maximum efficiency condition for each value of the field voltage corresponding to a certain gate position. The obtained curve is implemented as a look-up table in a microprocessor. The use of a microprocessor gives the flexibility for adjusting the curve locally with the implementation of the VSG controller on an actual VSG system. The block diagram in Fig.3.2 shows the subcontroller denoted as Efficiency-Maximizer where the look-up table needs to be processed (see Ref.1 for more detailed discussions on this subject). This block supplies an output signal corresponding to the target shaft-speed of the VSG system required to achieve maximum-efficiency operating conditions under varying pressure head and gate position.

In the laboratory set-up the armature voltage of the DC motor which simulates the turbine, is measured and fed as a signal to the microprocessor mentioned earlier. The reference signal of the field voltage of the DC motor is held fixed if the gate position is constant. A change in pressure head can be accomplished simply by a manual change of the reference signal of the armature voltage or by identifying this reference signal with a programmable profile of the varying conditions of the pressure head.

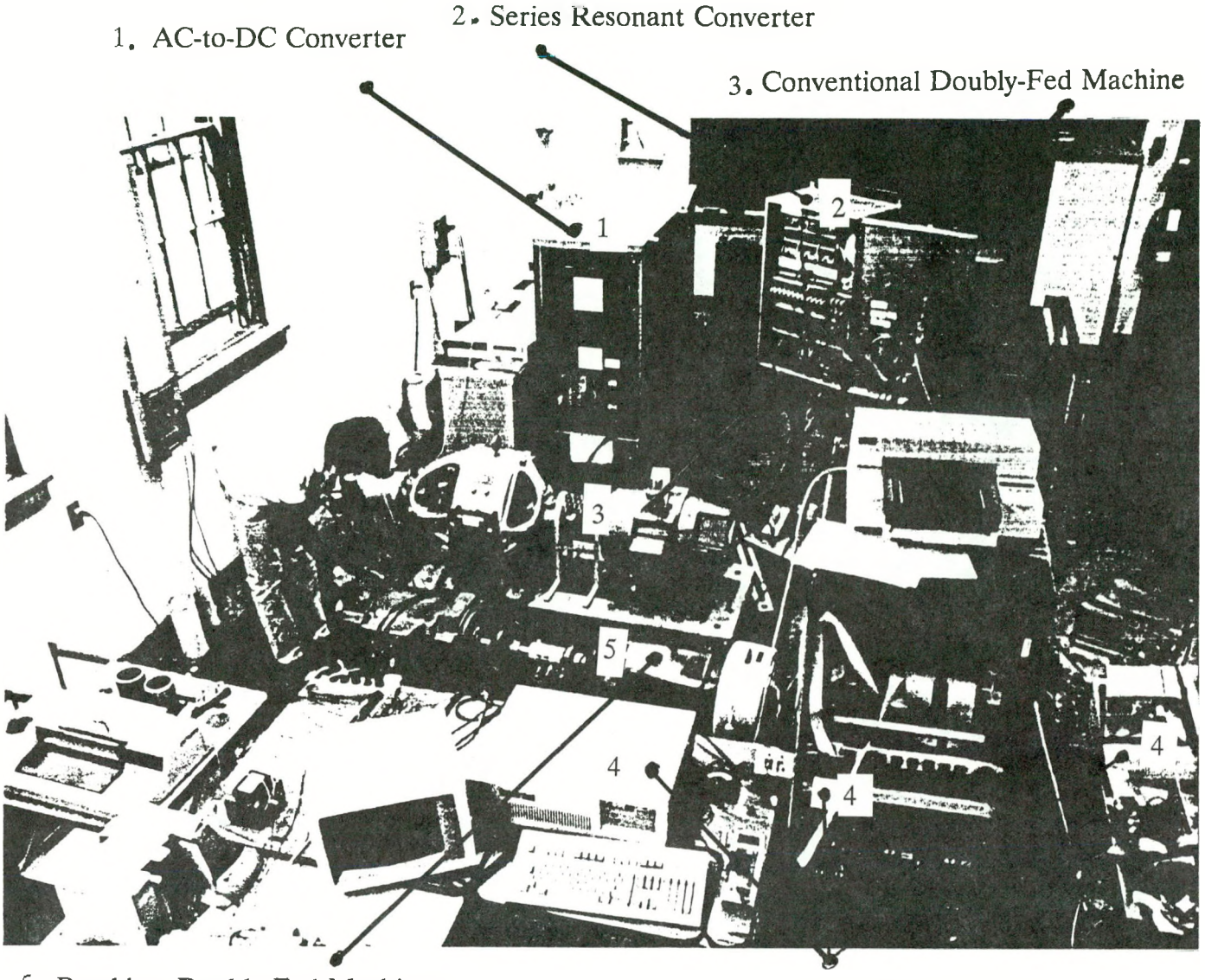

Fig.3.1 Variable-Speed Generation System at Oregon State University

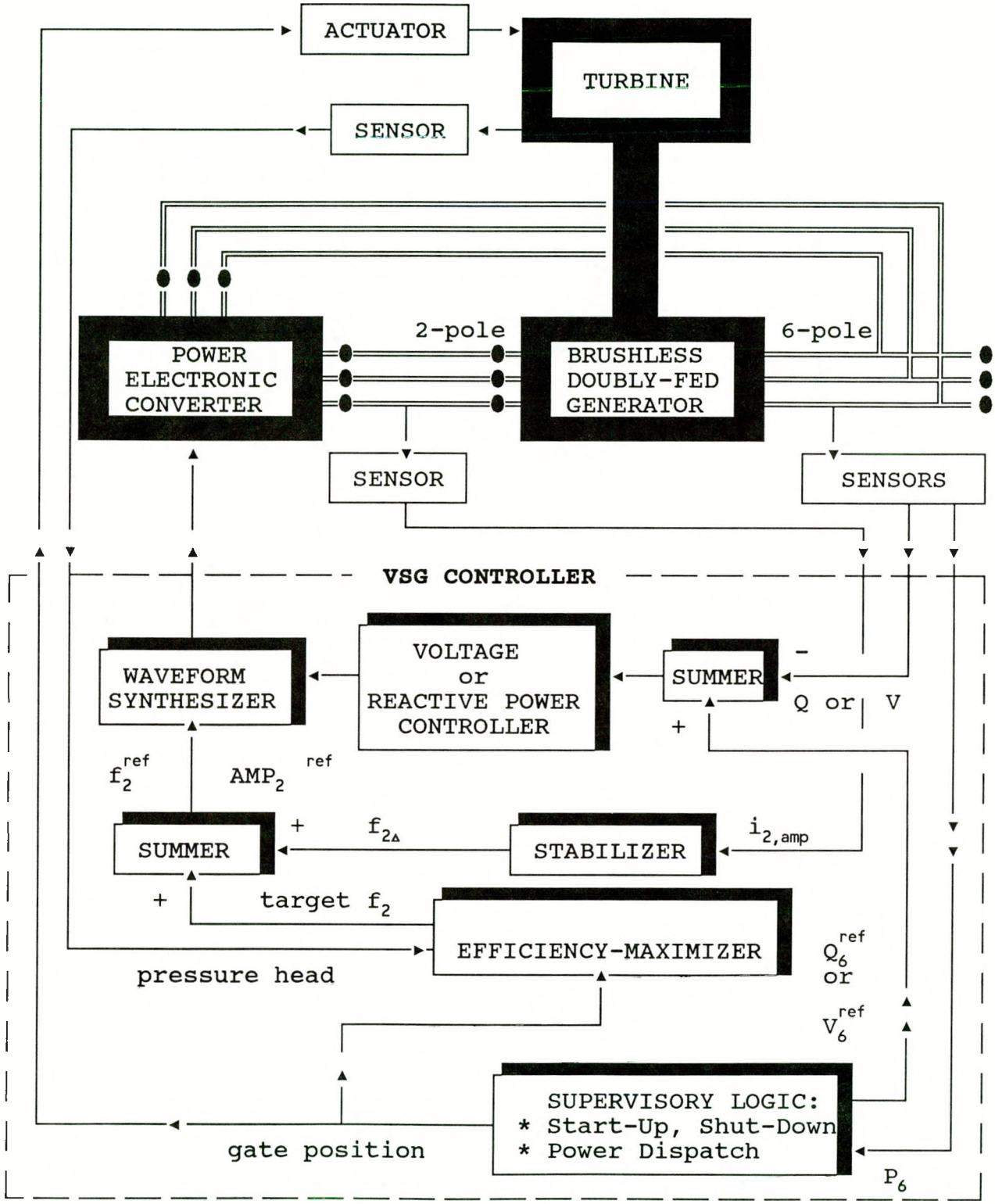

Fig.3.2 System Configuration of a Variable-Speed Generation (VSG) System

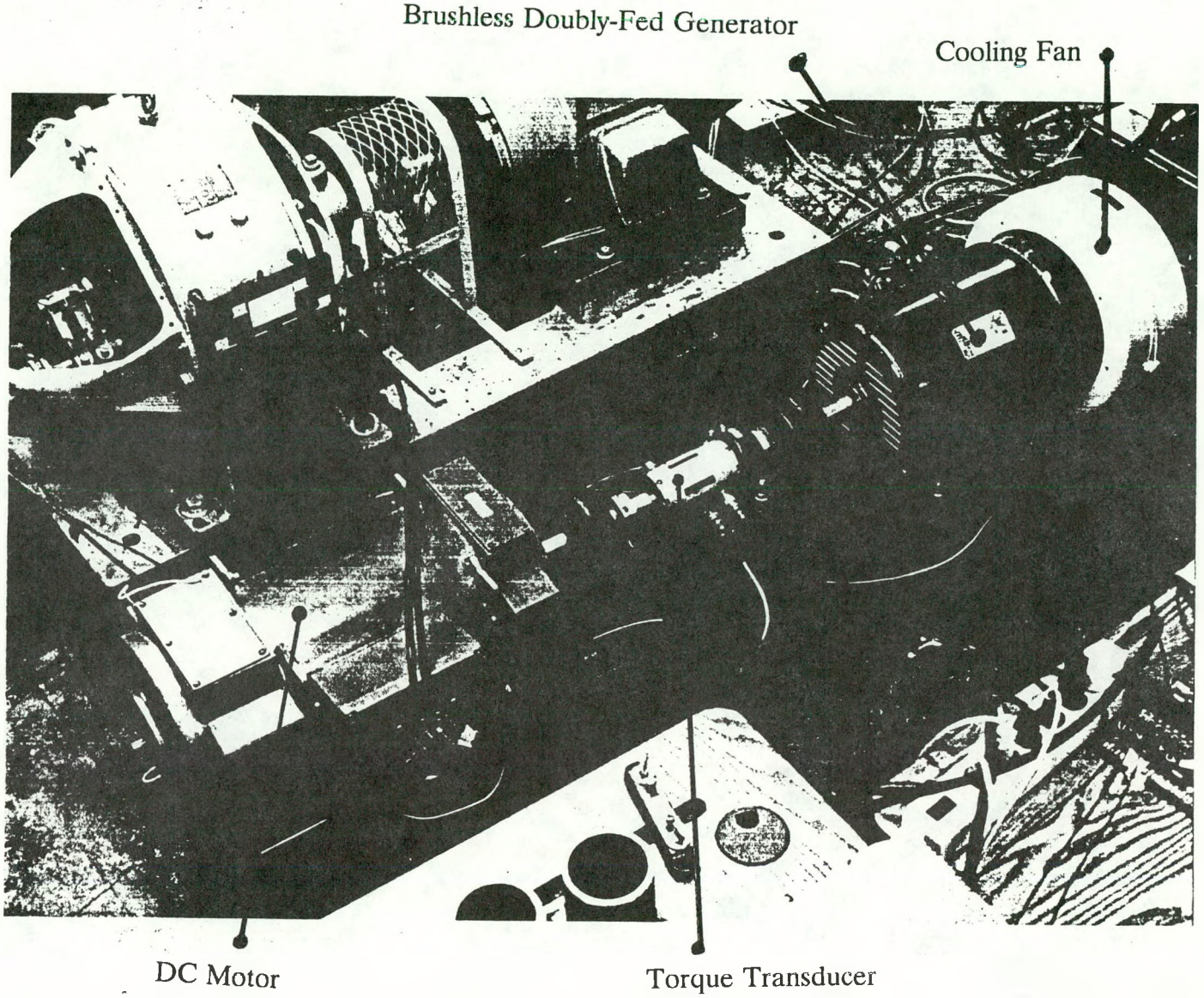

Fig.3.3 Close-up of the Brushless Doubly-Fed Generator

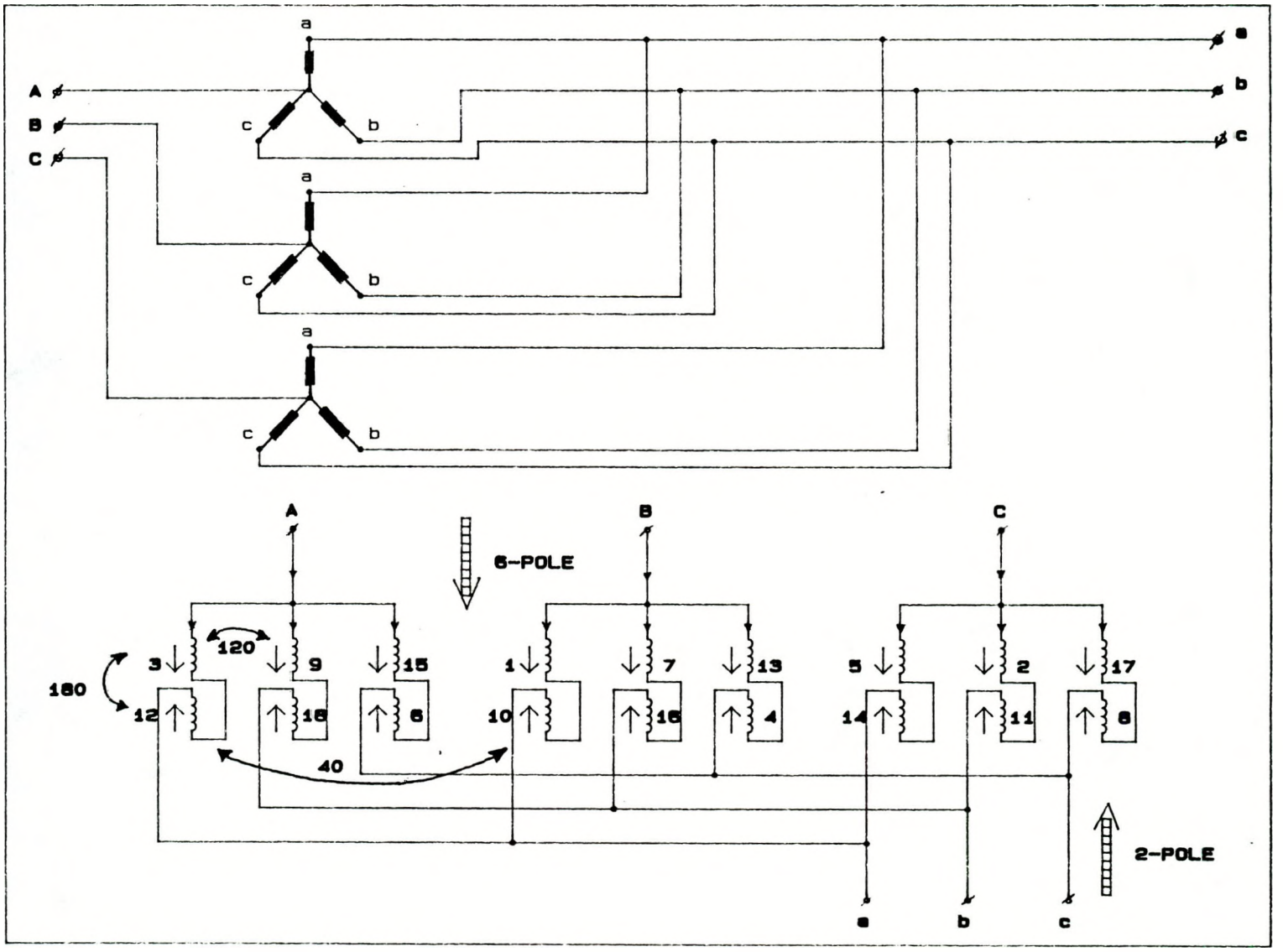

Fig.3.4 Wiring diagram of 2- and 6-pole stator 3phase systems with common windings

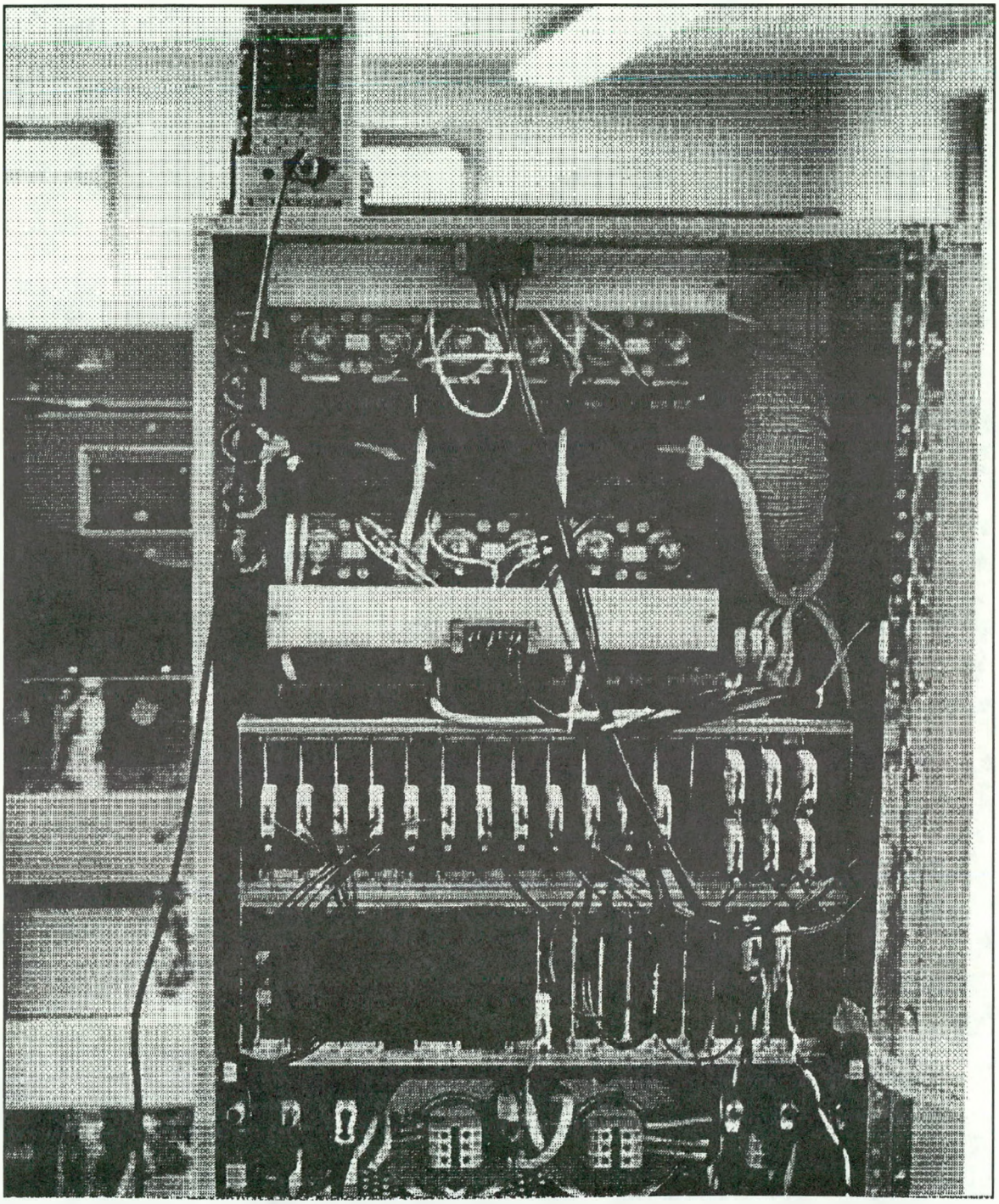

Fig.3.5 Close-up of the Series Resonant Converter

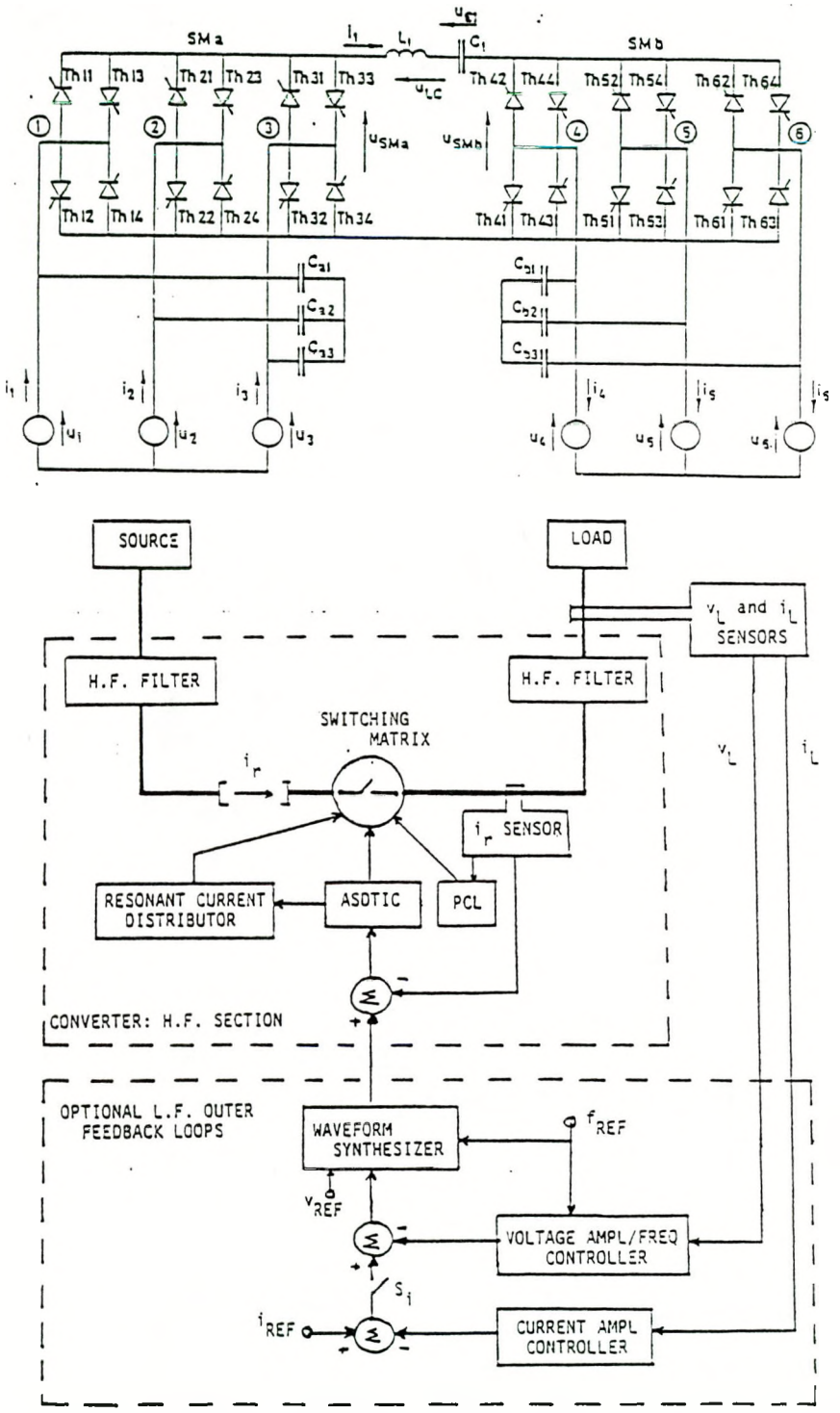

Fig.3.6 Power Circuit and Main Control Diagram of the 3-phase AC-to-AC Series Resonant Converter.

4. VSG CONTROLLER

The design of the controller for a VSG system using a conventional doubly-fed generator (with brushes and slip rings) was documented in detail in Ref.1 and 3. The chosen control structure and elements as well as the protection logic were generally preserved for the VSG system studied under this agreement, i.e. a VSG system using a brushless doubly-fed generator.

Some of the more relevant aspects will be briefly reintroduced for the reader's convenience. However, the focus will be on the subcontrollers, which are obviously different than the ones used for the conventional VSG system.

4.1 CONTROLLER'S STRUCTURE

As shown in Fig. 4.1 (reproduced from Fig. 3.2 for the reader's convenience), the VSG controller can be perceived to be hierarchically structured according to the following two levels:

(1) The local controller consists of three parallel subcontrollers which execute the tasks of: (1) voltage or reactive power control; (2) stabilizing the brushless doubly-fed generator; and (3) maximizing efficiency of the energy-conversion process. These subcontrollers supply information regarding the amplitude and frequency of the waveform which is synthesized by the waveform synthesizer. The output of the synthesizer is used as the reference signal for the output current or output voltage of the power electronic converter.

(2) The supervisory controller determines the target state of the VSG system as desired by the power dispatcher or on the basis of other important operator decisions such as start-up, shut-down, on/off logic for constant output power, on/off logic for the

efficiency maximizer, increase/decrease in output, etc.

The supervisory controller including the system protection logic requires logic and control elements which are not dependent on the type of generator used. Therefore, as far as the supervisory control and protection logic is concerned, reference is made to the logic as developed earlier for the work reported in Ref.3.

The local controller is obviously most critical to the operation of the VSG system. As explained in the INTRODUCTION to this report, emphasis of the work during the course of this contract is out of necessity on the stabilizer. With the exception of the efficiency maximizer, malfunction of any of these subcontrollers requires a system shut-down. Turning off the efficiency maximizer merely results in the VSG system operating at a shaft-speed which can be arbitrarily set by the operator. Effectiveness of the efficiency maximizer is strongly dependent on the efficiency characteristics of the prime mover (see Ref.1). In fact, the energy gain to be expected from a VSG system originates from the possibility of maximizing the efficiency of the prime mover by operating at varying shaft-speed as the primary resource condition varies. As far as the generator is concerned, only precautions need to be taken which should minimize the current demand while operating at these varying shaft-speeds. This was explained to be automatically taken care of by operating the generator with moderate or zero reactive power output. In view of these explanations, the efficiency maximization logic which was proposed in Ref.1 (page 26) and applied to a conventional VSG system, can be expected to be effective as well if the VSG system is equipped with a brushless doubly-fed generator.

A schematic diagram of the signal processing elements of the VSG controller is shown in Fig. 4.2. Connecting lines provided with a single arrow represent one-way communication channels between the units. Arrows going both ways show two-way communication channels between the units. The shown seven elements have the following functions.

(a) Data Acquisition System. This element contains all the required sensors as

indicated in Fig. 4.1. The Watt transducers used are Ohio Semitronics P Series Variable Frequency Watt Transducers. These transducers have a frequency range from DC to 500 Hz and a response time of less than 50 μsec, thus assuring accuracy at higher frequencies and with higher harmonics. The voltage transducers are all Ohio Semitronics VT Series Voltage Transducers. The voltage transducers which are used in the control loop provide an output signal that is directly proportional to the instantaneous value of the input. Other voltage transducers provide a DC output that is proportional to the rms value of the input signal. The instantaneously responding current transducers have a frequency range from DC to 5 kHz and a response time of 50 μsec. The current transducers are Ohio Semitronics CT-L Series Transducers with CTA Series Signal Conditioners. This combination also provides a frequency range from DC to 5 kHz. The outputs of a set three-phase current transducers on the 2-pole stator circuit are sampled and held by sample-and-hold amplifiers that are triggered by a common trigger pulse. This would provide instantaneous current amplitude values that are all obtained at precisely the same instant in time for the calculation of:

$$i_{ampl} = [i_a^2 + i_b^2 + i_c^2]^{1/2}$$

A less costly approach at an acceptable reduction of accuracy was found to be the sequential use of one D/A converter with a conversion speed of 20 μsec. In this case, the three individual phase currents are sequentially fetched and stored before the above formula is applied.

(b) General Purpose Controller. The controller is a Reliance Automate 40, which is based on the Motorola 68008 microprocessor and provided with 8 input and 8 output channels, as well as A/D converters. This controller is used with the system for development purposes only. Due to its general nature, unnecessary overhead on the processing time is significant, but the built-in PID loops, diagnostics and data base management capabilities are convenient tools for developing and testing the desired control logic. This controller is bypassed completely in the final stages of the design.

(c) Input Multiplexer. This element is an INTEL ISBX 311 and is capable of

accommodating 18 channels. The sampled analog signals from the Data Acquisition System are supplied to this multiplexer and are made ready for selective processing by a signal processing unit. Sampling of the channels and holding their value is carried out on this module. The sampling is performed on a single channel at a time with a sampling periodicity of 50 μsec per channel.

(d) Single-Board Computer. The INTEL ISBC 286/12 was chosen to serve as the high-speed signal processing element in previous versions of the VSG controller (see Ref.3). The computer is a high-speed, real time, 16-bit microprocessor including the A/D converters as well as the sockets of EPROMS on which the user's logic can be programmed. This board is obviously meant to house the control logic of the VSG's local controller (see Fig. 4.1), as well as all transfer functions of the subcontrollers and the look-up table of the efficiency-maximizer. However, all of the developed software could be fitted into the same processor of the IBM PC/AT which in Fig. 4.2 is already indicated to be needed for the supervisory logic. A commercially available input multiplexer and output demultiplexer was purchased which could be readily inserted on a socket of the PC/AT. The total processing time is not unacceptably increased. Aside from a significant reduction in the cost of the controller, a more flexible environment for the development of the controller is established. Programming, testing and modifications as well as control parameter adjustments without the need for the time-consuming burning of EPROMs can be conveniently done from the keyboard of the PC.

(e) Floating-Point Processor. This element, the INTEL NDP 80287, is necessary to obtain the accuracy of the calculations associated with the recursive equations generated by the transfer functions. The use of this processor is particularly helpful if extremely small increments are dealt with, such as when a steady-state condition is approached following a transient swing of a variable subjected to a lag network.

(f) Supervisory Computer. The IBM PC/AT was found to be adequate to perform the tasks of the supervisory controller as described earlier, including the capability of providing

diagnostics, execute protection logic and monitoring certain quantities which are important to the VSG system operator. Performance speed is not as important as with the single-board computer. In certain cases a delay needs to be introduced, such as to facilitate a gradual shut-down to minimize wear and tear, and to assure decoupled control with the subcontrollers of the local controller.

(e) Output Demultiplexer. This element is the last signal processing element in the VSG controller loop which started with the Data Acquisition element. The INTEL ISBX 328 containing the D/A converters and 8 channels was used for compatibility with the chosen single-board computer. The Output Demultiplexer provides the series-resonant converter with the reference signals for the amplitude and frequency of the converter's output voltage if the converter is operated in the voltage-source mode, or of the converter's output current if the converter is operated in the current-source mode.

4.2 STEADY-STATE STABILITY

The steady-state stability aspects of the brushless doubly-fed machine have been analyzed and reported in Ref.6. and will be reviewed here before a control logic will be presented which would assure that the machine operates within the steady-state stability limits, irrespective of changes to the prime mover conditions (or load if the machine runs as a motor).

A loss of synchronism will result if the steady-state stability limits are exceeded, even if only gradual changes are made to the prime mover. This phenomenon is known to occur with conventional doubly-fed machines (Ref.1) as well as with the well-known synchronous machines. Basically, a minimum amount of excitation current is needed in order to avoid a pull-out of synchronism. This minimum depends on the shaft-speed and the amount of power transferred through the machine. An additional peculiarity of the brushless doubly-fed machine is the need for this excitation current to be kept within some maximum value.

This maximum is likewise dependent on the shaft-speed and the amount of power transferred through the machine. It was explained in Ref.6 that the excitation current of the brushless doubly-fed machine is the current flowing in the stator 3-phase systems with the lower number of poles. Thus, the excitation current for the machine as studied under this agreement is the 2-pole current. The other set of 3-phase stator system is a 6-pole and carries the armature current. The 2-pole stator terminals are connected to the power electronic converter by which adequate control of the required excitation current is made possible.

In Ref.6, a tool of analysis denoted as the circle diagram method was presented which makes it possible to project the operating conditions of the synchronous mode. Any operating condition corresponds with an "operating point" in a 2-dimensional space, and, vice versa, the location of an operating point on the diagram completely characterizes the mode of operation, i.e. the amount of active and reactive power, the rms value and phase angle of both the 2-pole and 6-pole currents, the power factor, the electromagnetic torque produced (or the air-gap power), and the torque angle.

This diagram is shown in Fig. 4.3, where point A, for example, represents an operating mode. Projection of this point on the horizontal axis represents the active power P and on the vertical axis the reactive power Q generated or absorbed by the 6-pole 3-phase stator system. The angle Ψ, the currents I_{e1} and I_2 indicated on the diagram correspond to respectively, the power factor angle of the 6-pole system, the 6-pole current and the 2-pole current. Operating the machine such that the torque (or air-gap power) is held constant while changing any of the other possible variables of the machine, the operating point A will follow a trajectory which is a circle with point M as center. For constant 2-pole current, the trajectory point A is a circle with point N as center. The coordinates of point M and N are derived in Ref.6 and are dependent on the machine parameters (resistances and reactances) as well as the shaft-speed.

The circle diagram method provides a way to understand and predict the steady-state

stability limits of the brushless doubly-fed machine (Ref.6). In order to assure steady-state stable operation, the 2-pole current is restricted to have rms values between a minimum and maximum value. It was explained that the region bounded by these limits :

- decreases with increasing shaft-speed, and
- increases with increasing torque applied to the shaft (or increasing air-gap power).

It was also explained in Ref.6 that steady-state stability (synchronism) is lost if the 2-pole current is not kept within this region because of the lack of intersection of the 2-pole current circle and the air-gap power circle in the circle diagram. Therefore, the region of steady-state stability can be projected in the circle diagram.

These findings suggest that the circle-diagram method is not only a convenient tool of analysis for understanding the machine performance, but also can be used in a control scheme to assure steady-state stable operation. A steady-state stability stabilizer could be implemented which tracks the trajectory of the operating conditions in the circle diagram. By means of the converter, the 2-pole current could then be controlled such that operation beyond the steady-state stability region is prohibited, irrespective of changing prime mover or changing shaft-speed conditions. However, implementation of such a control logic is too elaborate. More attractive from an implementation point of view as well from an operating point of view is to assure steady-state stability by means of a reactive power controller which controls the reactive power at the 6-pole terminals of the brushless doubly-fed machine. This will be discussed in the next subsection.

4.3 VOLTAGE AND REACTIVE POWER CONTROLLER

The brushless doubly-fed machine is capable of supporting the grid requirements for reactive power as well as voltage level. Reactive power and voltage level are actually related variables and both variables are controllable through the same driving function in the VSG system, i.e. the rms or amplitude of the excitation current. For the designed machine, the excitation current is the 2-pole current. If the reactive power demand from an electric grid

is high, then voltage levels at certain buses in the grid tend to sag. Vice versa, a voltage controller regulates a proper level of reactive power supplied or absorbed by the grid. Obviously, a power-flow analysis is the proper tool for a dispatcher to determine the grid's required voltage and reactive power.

As far as the VSG system is concerned, a choice for either voltage control or reactive power control was mentioned to be possible and is decided to be given as options to the user. Obviously, in applications where the grid short-circuit capacity is high, the user would opt for a reactive power control mode in order to reduce line losses. Otherwise, and particularly for stand-alone operation, the voltage control mode can be expected to be preferred. Both controllers are presented in Fig. 4.4.

The reactive power controller fulfills another role for the VSG system which is more crucial than merely satisfying the user's need for reactive power control capability. A fast-acting reactive power controller takes care of the requirement to operate the brushless doubly-fed machine in the steady-state stable region, irrespective of varying shaft speed or prime mover (or load if running as a motor) conditions. This was mentioned in the previous section and will be briefly explained here (see Ref.6 for more detail).

The stabilizing effect of the reactive power controller can be understood (predicted) by means of the circle diagram which captures the steady-state performance of the brushless doubly-fed machine. Stable steady-state operation is only possible if a circle representing constant torque (or air-gap power) operation intersects with a circle representing constant excitation current performance. Note that the excitation current is considered to be the 2-pole current. In considering the nature of the operating conditions of the brushless doubly-fed machine in the circle diagram of Fig. 4.3 (where point A is, for example, a particular operating point), it can be inferred that forcing the machine to operate with a constant 6-pole reactive power output would always provide the required intersection of a constant torque-circle and a constant excitation-circle. Therefore, irrespective of the amount of torque applied to the machine (or to be produced by the machine) and irrespective of the

shaft-speed, stable steady-state operation is assured if the controller is successful in maintaining constant 6-pole reactive power output. It is remarked that the steady-state stability margin is lower if the 6-pole system absorbs reactive power and that zero reactive power output is most preferable since in this case the machine runs with unity power factor at the 6-pole terminals. Note that the 6-pole system is considered as the armature of the machine.

The steady-state stabilizing effect of the reactive power controller which was predicted with the analysis (presented in Ref. 6) was confirmed with the implemtation as conducted during the course of this research contract. In order to increase the response speed of the reactive power controller as can be observed from Fig. 4.4, the integrator could be replaced by a lead-lag network well-known to those skilled in the art. Fig. 4.5 shows the steady-state stability limits for the 2-pole (excitation) current with the brushless doubly-fed machine driven by a prime mover with a cubic power-speed characteristic (hydro or wind turbine). The RPM can be calculated from the value of the slip s from the equation:

$$RPM = 60 * (1 - s) * f_{s1}/(N_1 + N_2) \qquad (4.1)$$

where N_1 and N_2 are the pole-pair numbers of the two sets of stator 3-phase systems and f_{s1} the supply frequency of the 3-phase system with N_1 pole-pairs.
With the 6-pole supply frequency equal to 60 Hz and the number of pole-pairs n_1 and n_2 respectively 1 and 3, this RPM is given by: RPM = 900 * (1 - s).

In Fig. 4.6, the effect of maintaining the 6-pole reactive power Q at zero (unity power factor) is a 2-pole current performance with values which are within the steady-state stability limits given in Fig. 4.5. This clearly demonstrates that:

(a) the circle diagram is a valid and powerful tool of analysis to synthesize and predict an adequate controller assuring stable steady-state performance,

(b) a fast acting reactive power controller assures stable steady-state operation. irrespective of varying shaft-speed and varying prime mover (or load) conditions.

4.4 DYNAMIC STABILIZER

Another stability phenomenon to be dealt with is the dynamic stability of the brushless doubly-fed machine. The steady-state stability aspect as discussed in the previous section does not take into consideration the effect of small disturbances which invariably occurs due to, for instance, fluctuations in the grid voltage or converter harmonics. These small disturbances may cause a stable steady-state operating mode to oscillate and in the worst case, to cause a complete loss of stability if synchronism is lost.

It is pointed out that in an operating region in which the system is dynamically stable, that the system is steady-state stable as well. The opposite is not true. The steady-state stability characteristics of the brushless doubly-fed machine could be predicted with the circle diagram method because the method is derived from the steady-state model of the machine (Ref. 6). Therefore, it is not possible to extract conclusive information from this method regarding the dynamic stability properties of the brushless doubly-fed machine.

The brushless doubly-fed machine was observed to suffer from such a dynamic stability problem in a small speed region around the slip value given by :

$$s = \frac{N_2}{N_1 + N_2} , \qquad (4.2)$$

where N_1 and N_2 are the pole-pair numbers of the two sets of stator 3-phase systems with $N_1 > N_2$. The RPM value follows from Eqn. (4.1). For the designed machine with $N_1 = 3$ and $N_2 = 1$, this dynamic instability region is at about 525 RPM to 675 RPM.

4.4.1 DYNAMIC STABILIZER WITH CURRENT FEEDBACK

A literature search pointed to a paper by Cook and Smith (Ref. 7) where the existence

of such a dynamic instability region was reported with their computer study of a system consisting of two induction machines with a common rotor. Such a system could be considered a simplified version of the brushless doubly-fed machine. It is reasonable to expect that certain performance features of this system would apply as well to those of the brushless doubly-fed machine, even though the brushless doubly-fed machine is designed with a single stator containing common windings for two sets of 3-phase stator windings. In the study by Cook and Smith a dynamic model was used and an eigenvalue analysis reveals a shift of the eigenvalues to the right-half plane of the complex domain if indeed the system is operated in the region given by Eqn. (4.2). It was also concluded that a feedback of the DC-link current of the converter used in their study to control the frequency of one of the induction machines is effective in resolving the dynamic stability problem.

For the VSG system in the laboratory, a series-resonant converter is used rather than a DC-link converter. A similar feedback as proposed by Cook and Smith can be realized by feeding back the amplitude of the current of the 2-pole stator system which is connected to the converter. This signal is obtained simply by sensing the 3 output phase currents from which the amplitude is obtained by applying the relationship:

$$i_{2,amp} = \mathrm{SQRT}[(i_{2a})^2 + (i_{2b})^2 + (i_{2c})^2] \quad . \qquad (4.3)$$

This amplitude signal is shown in Fig. 4.1 to be supplied as an input to the stabilizer. The stabilizer output signal $f_{2\Delta}$ is provided as an additional signal for the reference signal of the converter output frequency. Note that this signal is added to the target frequency signal produced by the efficiency maximizer and obviously is meant to instruct the VSG system to run with some shaft-speed by which maximum-efficiency operation is assured. This signal is constant if the resource condition is steady. The stabilizer signal can be expected to be oscillatory since the purpose of the stabilizer is to counteract the oscillations due to the instability phenomenon. These undesirable oscillations are in essence assumed to be detectable from the oscillations in the amplitude of the 2-pole current.

The stabilizer's structure in terms of transfer functions is given in Fig. 4.7 and can be observed to form a pass-band filter consisting of 3 elements:

(1) a low-pass filter to cut off the effect of high-frequency noise (with time-constant τ_1),

(2) a "wash" term to deactivate the stabilizer if no unwanted oscillations occur due to dynamic instability,

(3) A high-pass filter to pass through the oscillation frequency f_{osc} which needs to be "battled" by the stabilizer (with time-constant τ_2).

The combined effect of these elements is shown in the gain and angle Bode diagrams of Fig. 4.7 which obviously reflect the characteristics of a band-pass filter with two cut-off frequencies f_1 and f_2. Note that these cut-off frequencies are related to the time-constant τ_1 and τ_2 according to the relationships:

$$f_1 = \frac{1}{2\pi\tau_1} \qquad \text{and} \qquad f_2 = \frac{1}{2\pi\tau_2} \quad . \qquad (4.4)$$

Adequate values for the stabilizer parameters, i.e. f_1, f_2 and K, could be determined on the basis of the following considerations. The unwanted frequency f_{osc} could be experimentally verified and counteracting this effect would require f_{osc} to be positioned in a band bounded by f_1 and f_2. This is shown in the gain diagram of Fig. 4.7. The gain K as the third stabilizer parameter determines in essence the sensitivity of the stabilizer. Fig. 4.7 also shows the phase angle between the stabilizer's input and output signals which indicates that this stabilizer would attempt to counteract the oscillations of the 2-pole current amplitude with practically no delay (phase angle is about zero at the value of the oscillation frequency).

The stabilizer feedback loop requiring only current sensors to provide the 2-pole current amplitude as an input signal to the stabilizer is elegant in that no tachometer is needed and, therefore, stabilization could be considered an effort restricted to the control domain of the converter. However, effectiveness of this control needs to be verified. This stabilizer with

the discussed procedure for determining its parameters will be adequate only if the oscillations in the 2-pole current amplitude indeed represent the shaft-speed oscillations due to the instability phenomenon. In other words, effectiveness depends on the lack of a significant phase angle discrepancy between the oscillation in the amplitude of the 2-pole current and that in the shaft-speed. It can be remarked that the occurrence of such a phase angle discrepancy could still be compensated to same extent by adjusting the corner frequencies f_1 and f_2. However, to find the correct amount of phase angle compensation can be expected to be difficult due to the nonlinear phase angle curve to be dealt with in the band region.

4.4.2 DYNAMIC STABILIZER WITH SPEED FEEDBACK

Rather than the 2-pole current amplitude, the shaft-speed could be used as the feedback signal for the dynamic stabilization of the machine. In this case a signal proportional to the RPM of the machine shaft is the input signal to the stabilizer shown in Fig. 4.8. As opposed to the stabilizer with a current feedback (see discussion in the previous subsection), a stabilizer with speed feedback counteracts the oscillations due to the instability problem directly. No phase angle compensation efforts will be needed and, as will be clear during the course of the further discussions, this stabilizer causes the brushless doubly-fed machine to obtain extra non-dissipative damping. Fig. 4.8 shows that the stabilizer structure and elements are the same as those for the stabilizer with a current feedback in Fig 4.7. However, the parameters of the stabilizer needs to be chosen quite differently.

The effect of the stabilization control could be analyzed from a complete dynamic model of the VSG system. However, since relatively small disturbances are of interest and since multi-kilowatt machines have a relatively high rotor moment of inertia, it is reasonable to assume that the dynamics of the electrical variables are so much faster that a decoupled treatment of the electrical and mechanical variables is practically justified. Such a view in the design of controllers for electromechanical energy converters has been successfully

applied in many other applications and is known as incremental-motion analysis (Ref. 10). In this analysis, equations are derived which are only valid for incremental motions and boils down to the linearization of the dynamic equations around steady-state operating conditions. Without such an approach, the design of the controller is quite complex and has to be based on a set of non-linear multi-dimensional differential equations. For all practical purposes, a controller designed on an incremental-motion basis can be just as effective (Ref. 10). Moreover, since stabilization of the shaft-speed is desired, a dynamic analysis confined to the inertial system of the system can be expected to yield a controller which will be effective in counteracting the shaft speed oscillations associated with the instability problem.

Consider first the inertial system of a conventional synchronous machine. The torque equation governing the dynamics of the inertial system is given by:

$$J \frac{df_{m\Delta}}{dt} = T_{m\Delta} - T_{e\Delta} , \qquad (4.5)$$

where: T_m = mechanical torque applied to the synchronous machine,
T_e = torque of electromagnetic origin produced by the synchronous machine,
f_m = shaft speed expressed in mechanical rad/sec (RPM = $60f_m$),
J = rotor moment of inertia.

Note that the torque equation here is presented in its incremental form, i.e. it only captures the incremental dynamic performance of the system with respect to some steady-state operating condition.

The electromagnetic torque T_e is proportional to product terms of stator and rotor currents, but in steady-state can be derived to be a transcendental function of the torque angle δ. This angle is the angle between the stator and rotor rotational fields.
The machine running in steady-state and converting some amount of mechanical power into electric power causes the torque angle δ to assume some constant value. If the machine is in a dynamic state, the machine would not run synchronously and a discrepancy between

angular speeds of the stator and rotor rotational fields would result. Therefore, in this case the torque angle δ will be varying.

For incremental motion associated with relatively small disturbances, and neglecting saliency effects of the machine (which would add an additional term dependent on 2δ), the electromagnetic torque can be proven (Ref. 10) to satisfy the relationship:

$$T_{e\Delta} = \frac{\delta_\Delta}{C} + D\frac{d\delta_\Delta}{dt} \quad , \tag{4.6}$$

with C and D being constants depending on the machine parameters, the machine EMF and the voltage of the electric utility grid to which the machine is connected. Assuming that the machine stator is connected to a 60 Hz electric utility grid, the torque angle δ follows from:

$$\frac{d\delta}{dt} = f_m - \frac{60}{N} \quad , \tag{4.7}$$

where N is the number of pole-pairs and δ expressed in mechanical radians. for incremental motion, this equation reduces to :

$$\frac{d\delta_\Delta}{dt} = f_{m\Delta} \qquad \text{and hence,} \qquad \delta_\Delta = \int f_{m\Delta}dt \quad . \tag{4.8}$$

Substituting $T_{e\Delta}$ from Eqn. (4.6) into the torque equation of Eqn. (4.5), and subsequently substituting into the result the relationships given in Eqn. (4.8), yield the torque equation:

$$J\frac{df_{m\Delta}}{dt} + D\,f_{m\Delta} + \frac{1}{C}\int f_{m\Delta}dt = T_{m\Delta} \quad . \tag{4.9}$$

This result demonstrates that the dynamics of the inertial system is equivalent to the

dynamics associated with an electric circuit containing a resonant circuit as shown in Fig. 4.9. The rotor moment of inertia J is an inductor, the constant C is a capacitor and the damping factor D the resistance in the circuit. The applied torque $T_{m\Delta}$ and the shaft-speed $f_{m\Delta}$ are respectively the voltage source and the current flowing in the circuit. Hence, the natural frequency of the inertial system and the amplitude of shaft-speed oscillations due to a disturbance can be quickly determined to be respectively :

$$\omega_n = \frac{1}{\text{SQRT}(JC)} \qquad \text{and} \qquad \text{Max}(f_{m\Delta}) = \frac{T_{m\Delta}}{\text{SQRT}(J/C)} \quad . \qquad (4.11)$$

In conclusion, this analysis on the dynamics of the inertial system of a conventional synchronous machine provides an insight into to the effect of the different machine parameters. It shows that a disturbance would cause oscillations in the torque angle and the shaft-speed and the extent of these oscillations is transparent from the result given in Eqn. (4.11). Obviously, these oscillations are not acceptable if the damping factor D is insignificant. Normally, with synchronous machines, sufficient damping is present and often synchronous machines are provided with damper bars to establish an extra margin of damping.

A similar incremental-motion analysis could be performed for the brushless doubly-fed machine. Eqn. (4.5) is a torque equation which applies to electric machinery in general. A torque angle δ could also be introduced for the brushless doubly-fed machine which conceptually is the same torque angle as that of a conventional synchronous machine. In fact, it was mentioned earlier that only the synchronous mode of operation of the brushless doubly-fed machine is of concern. The induction mode is only allowed if synchronism is lost. Consequently, the electromagnetic torque of the brushless doubly-fed machine will exhibit the same dependence on the torque angle as given in Eqn. (4.6). However, let's consider the worst case in that electromagnetic torque of the brushless doubly-fed machine does not contribute to any damping. In this case, the electromagnetic torque given in Eqn. (4.6) reduces to :

$$T_{e\Delta} = \frac{\delta_{\Delta}}{C} \quad , \tag{4.12}$$

where C is again some constant depending on the machine parameters, the machine EMF and the voltage of the electric utility grid to which the 6-pole stator 3-phase system is connected.

The torque angle δ for the brushless doubly-fed machine obviously does not follow from the same relationship given for the synchronous machine in Eqn. (4.7). The torque angle definition is more complicated due to the 3 frequencies and the associated 3 rotational fields involved with the conversion process. The 3 frequencies are:

f_6: the supply frequency to the 6-pole stator 3-phase system, which is a constant value since this system is directly connected to the electric utility grid (60 Hz),

f_2: the supply frequency to the 2-pole stator 3-phase system, which is accessible for control by means of the power electronic converter to which the 2-pole system is connected,

f_r : the rotor current frequency.

In the synchronous mode of operation of the brushless doubly-fed machine, these frequencies are related to each other according to (Ref. 6) :

$$f_r + \frac{N_6 - N_2}{2} f_m = \frac{f_6}{2} + \frac{f_2}{2} \quad , \tag{4.13}$$

with N_2 and N_6 respectively the number of pole-pairs of the 2-pole and 6-pole stator 3-phase systems. Since no direct control on the rotor-current frequency f_r is possible, let us eliminate f_r from this relationship by means of another relationship between f_r and f_2 (see Ref. 6) :

$$f_r = f_2 + N_2 f_m \quad . \tag{4.14}$$

Therefore, substituting f_r from Eqn. (4.14) into Eqn. (4.13) yields:

$$\frac{f_2}{N_2 + N_6} + f_m = \frac{f_6}{N_2 + N_6} \quad . \tag{4.15}$$

The result in Eqn. (4.15) indicates that synchronous operation requires a rotational field associated with the 2-pole excitation and rotating with a frequency given by the terms on the left-hand side of the equal sign, to be in synchronism with the 6-pole rotational field rotating with a frequency given by the term on the right-hand side of the equal sign. Hence, the torque angle δ follows from :

$$\frac{d\delta}{dt} = \left[\frac{f_2}{N_2 + N_6} + f_m \right] - \frac{f_6}{N_2 + N_6} \quad . \tag{4.15}$$

Since the supply frequency f_{s6} is constant (60 Hz in USA), this equation reduces for incremental motion to :

$$\frac{d\delta_\Delta}{dt} = \frac{f_{2\Delta}}{N_2 + N_6} + f_{m\Delta} \quad , \tag{4.16}$$

and hence :

$$\delta_\Delta = \int \left[\frac{f_{2\Delta}}{N_2 + N_6} + f_{m\Delta} \right] dt \quad . \tag{4.17}$$

Substituting this result into Eqn. (4.12) and subsequently substitution of Eqn. (4.12) into Eqn. (4.5) establishes the incremental torque equation of the brushless doubly-fed machine in terms of the shaft speed f_m and the controllable current frequency f_2 of the 2-pole stator 3-phase system as :

$$J \frac{df_{m\Delta}}{dt} + \frac{1}{C} \int f_{m\Delta} dt + \frac{1}{(N_2 + N_6)C} \int f_{2\Delta} dt = T_{m\Delta} \quad . \tag{4.18}$$

It is to be noted from this result how powerful the incremental analysis is. At this stage, it is immediately obvious as to what kind of control strategy could be applied in order to mitigate the effect of unwanted oscillations in the shaft speed f_m (remark: RPM = $60f_m$). The frequency f_2 is under control of the power electronic converter to which the 2-pole 3-phase stator system is connected. A most desirable control which leads to the introduction of extra damping to the inertial system in a non-dissipative manner, is obtained if the frequency f_2 is controlled such that :

$$f_{2\Delta} = K \frac{df_{m\Delta}}{dt} \qquad (4.19)$$

Under this control and , thus, by substituting $f_{2\Delta}$ from Eqn. (4.19) into Eqn. (4.18), the torque equation given in Eqn. (4,18) becomes:

$$J \frac{df_{m\Delta}}{dt} + \frac{1}{C} \int f_{m\Delta} dt + \frac{K}{(N_2 + N_6)C} f_{m\Delta} = T_{m\Delta} \quad . \qquad (4.20)$$

This result indeed demonstrates that the chosen control as given in Eqn. (4.19) leads to the introduction of a non-dissipative damping which obviously stems from the third term on the left-hand side of the equal sign in Eqn. (4.20). This is also clear from the electric analog representation of this equation as shown in the Fig. 4.9b where the factor of $f_{m\Delta}$ in the mentioned third term of Eqn. (4.20) is a resistance. J and C are respectively the inductor and capacitor in the circuit; $T_{m\Delta}$ and $f_{m\Delta}$ respectively the voltage source and current flowing in the circuit. It should also be noticed that the natural frequency of the inertial system is not effected by the proposed control. This is attractive since there is no need to adapt the corner frequencies for different values of the gain K. The gain K determines the sensitivity of the stabilizer.

Implementation of the proposed control reflected in Eqn. (4.19) with a pure

differentiator is clearly not advisable because of the noise level that the signal from the shaft-speed sensor is expected to be contaminated with. A viable approach is the use of a band-pass filter as was proposed for the stabilizer discussed in the previous subsection. However, the filter parameters consisting of the corner frequencies f_1 and f_2 as well as the gain K have to be chosen differently as shown in Fig. 4.8. The frequency f_1 is again chosen to cut off the effect of noise in the input signal $f_{m\Delta}$. The corner frequency f_2 is proposed to be taken equal to f_1 with the purpose of obtaining a wide band of 90-degree phase angle difference between input and output of the stabilizer. This requirement is imposed by the proposed control in Eqn. (4.19) since, in fact, the 90-degree phase angle difference warrants the desired differentiation. Moreover, both f_1 and f_2 have to be chosen to be significantly higher than the expected oscillation frequency f_{osc} associated with the stability problem. This warrants the phase angle difference to be 90 degrees at the oscillation frequency and in essence assures the effectiveness of the controller to provide non-dissipative damping for the unwanted oscillations.

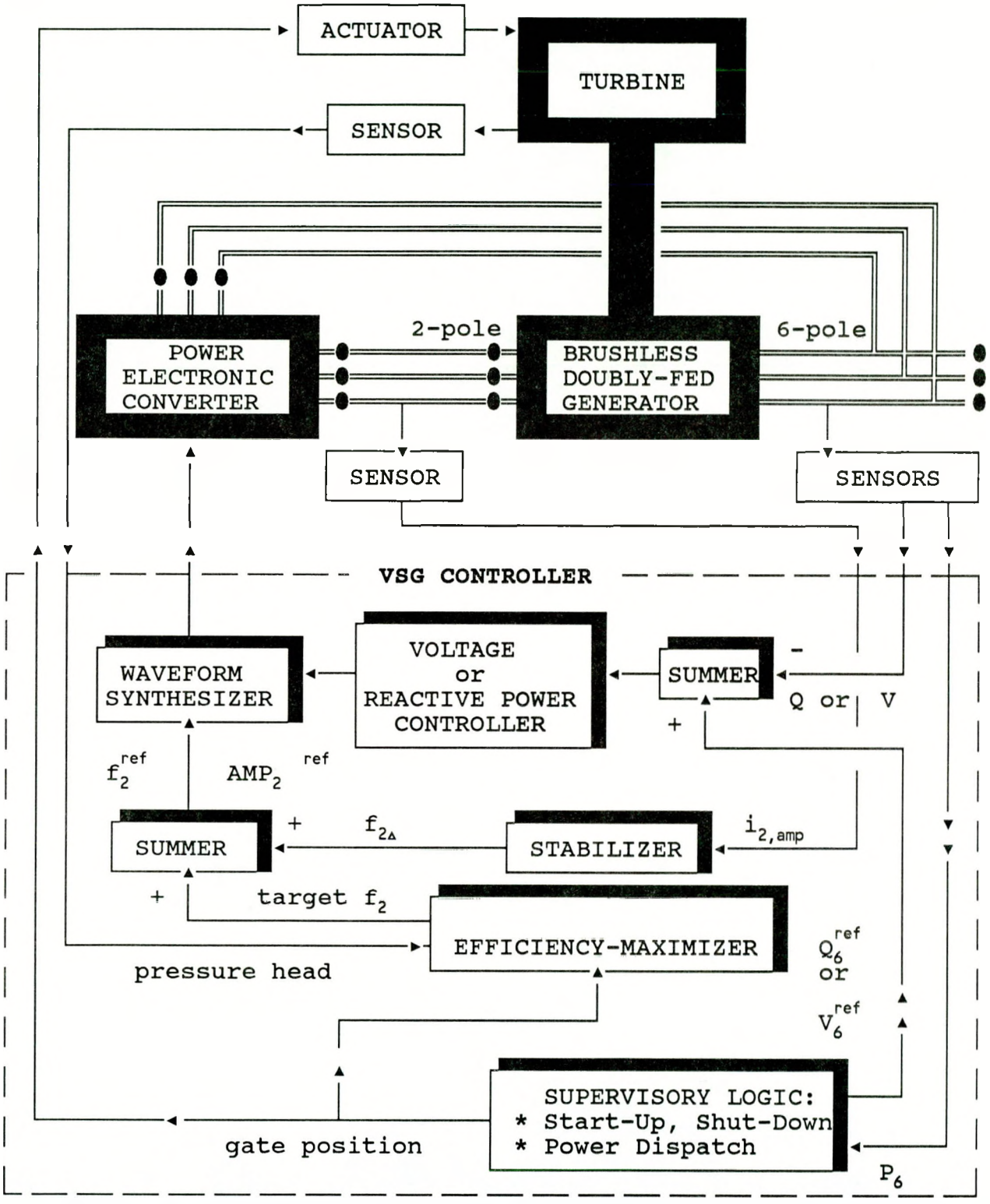

Fig.4.1 System Configuration of a Variable-Speed Generation (VSG) System

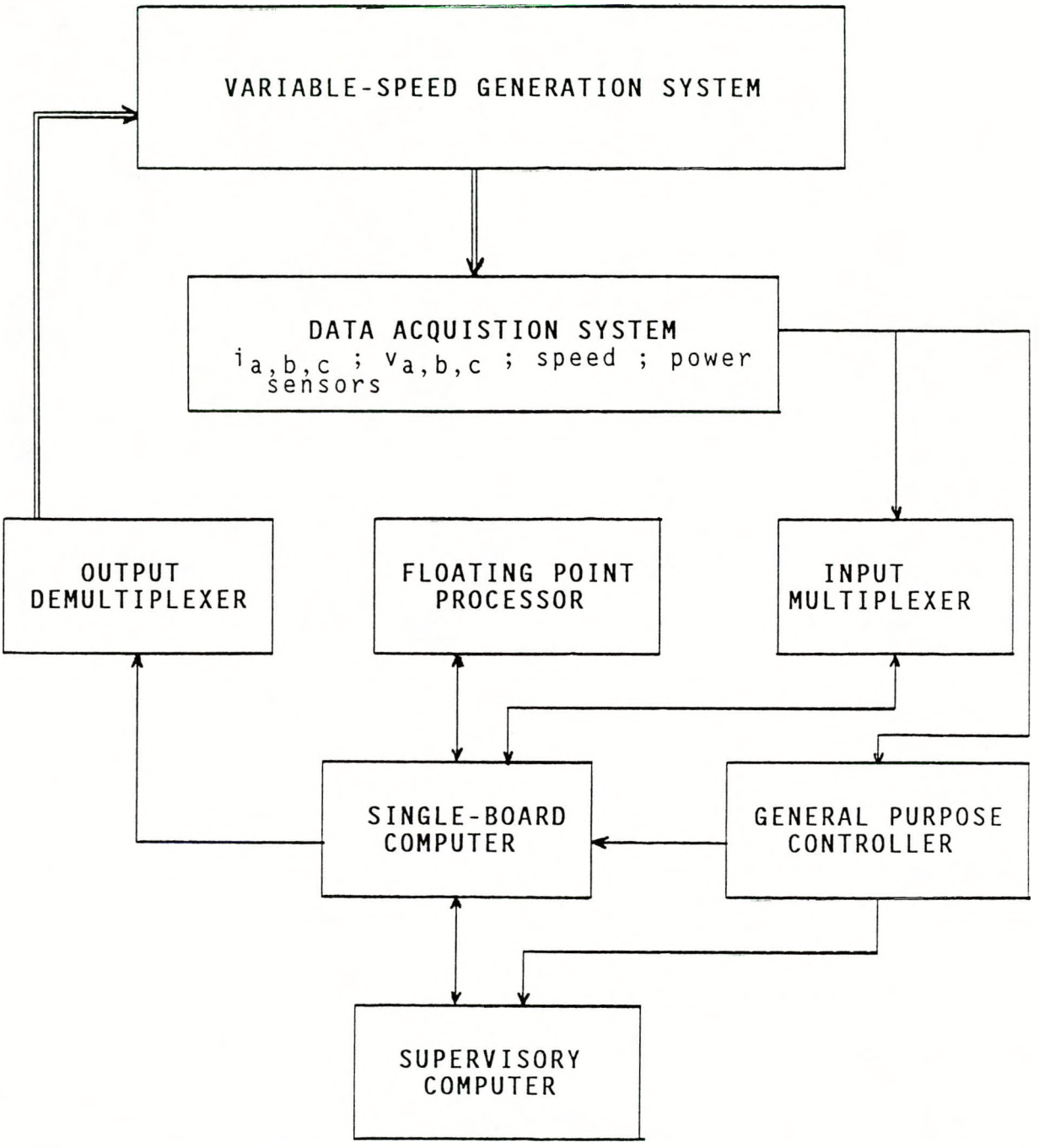

Fig.4.2. Control Elements of the VSG system

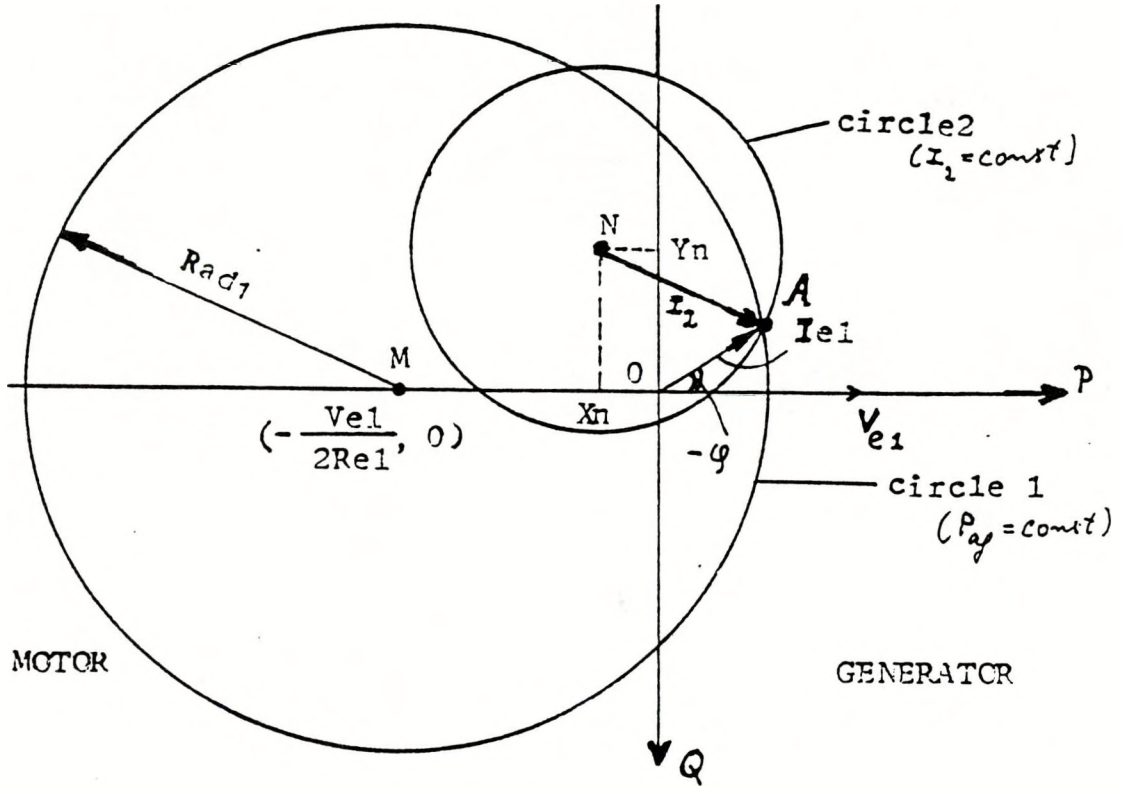

Fig. 4.3 Operating mode of the brushless doubly-fed machine as reflected in a circle diagram

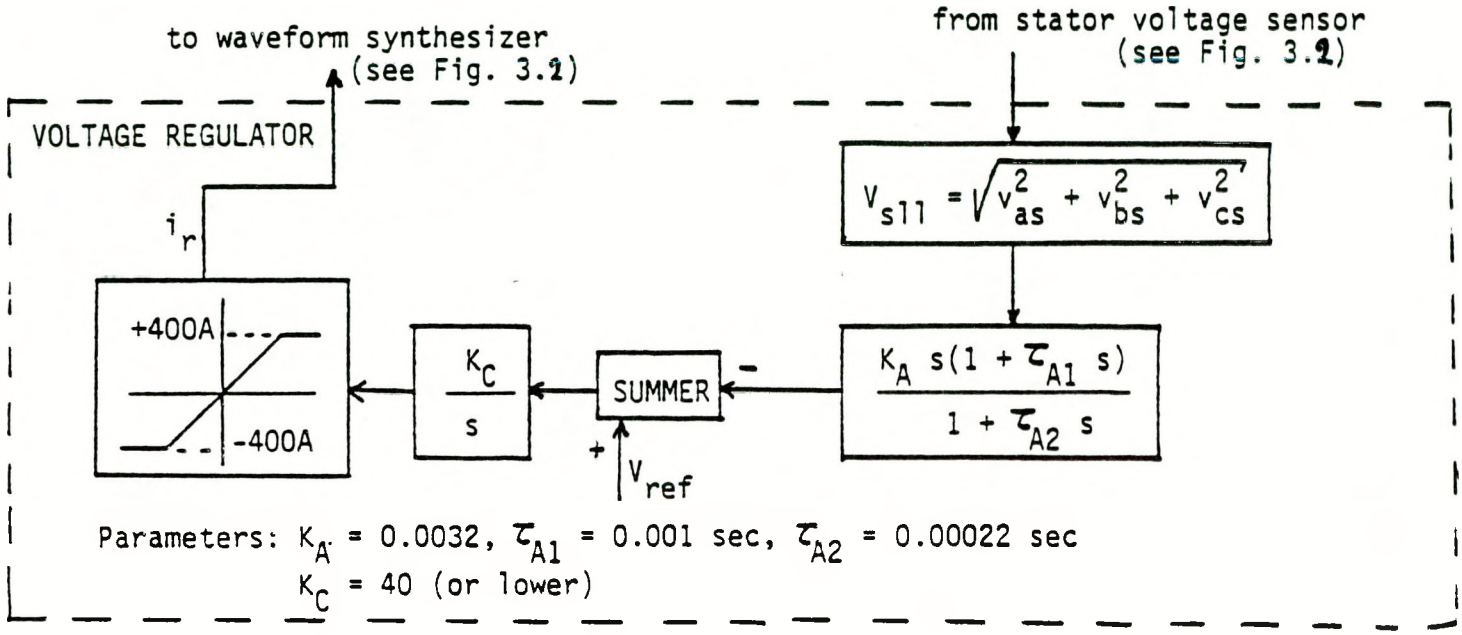

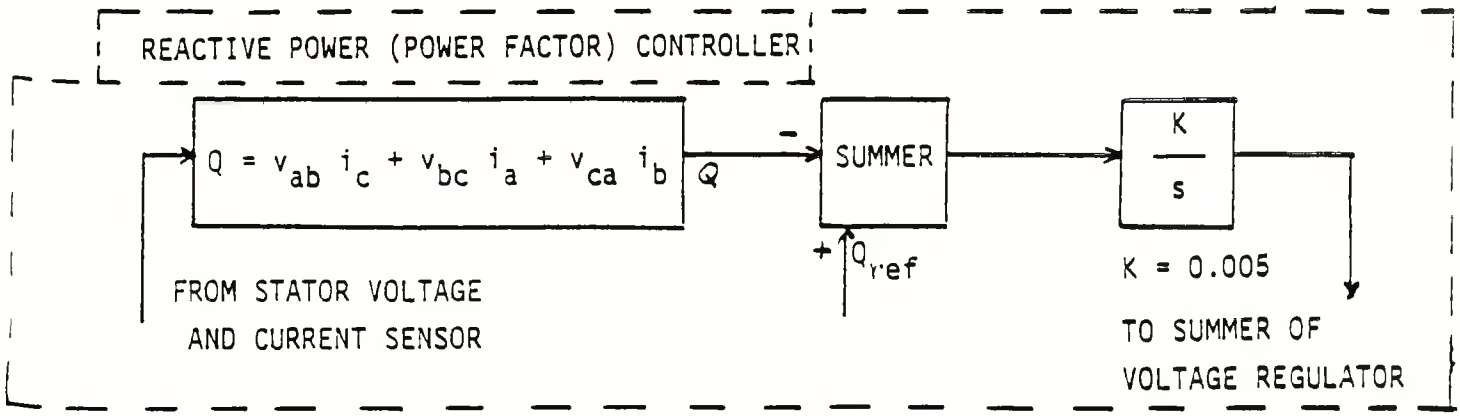

Fig.4.4 Voltage and Reactive Power Controller for a VSG system

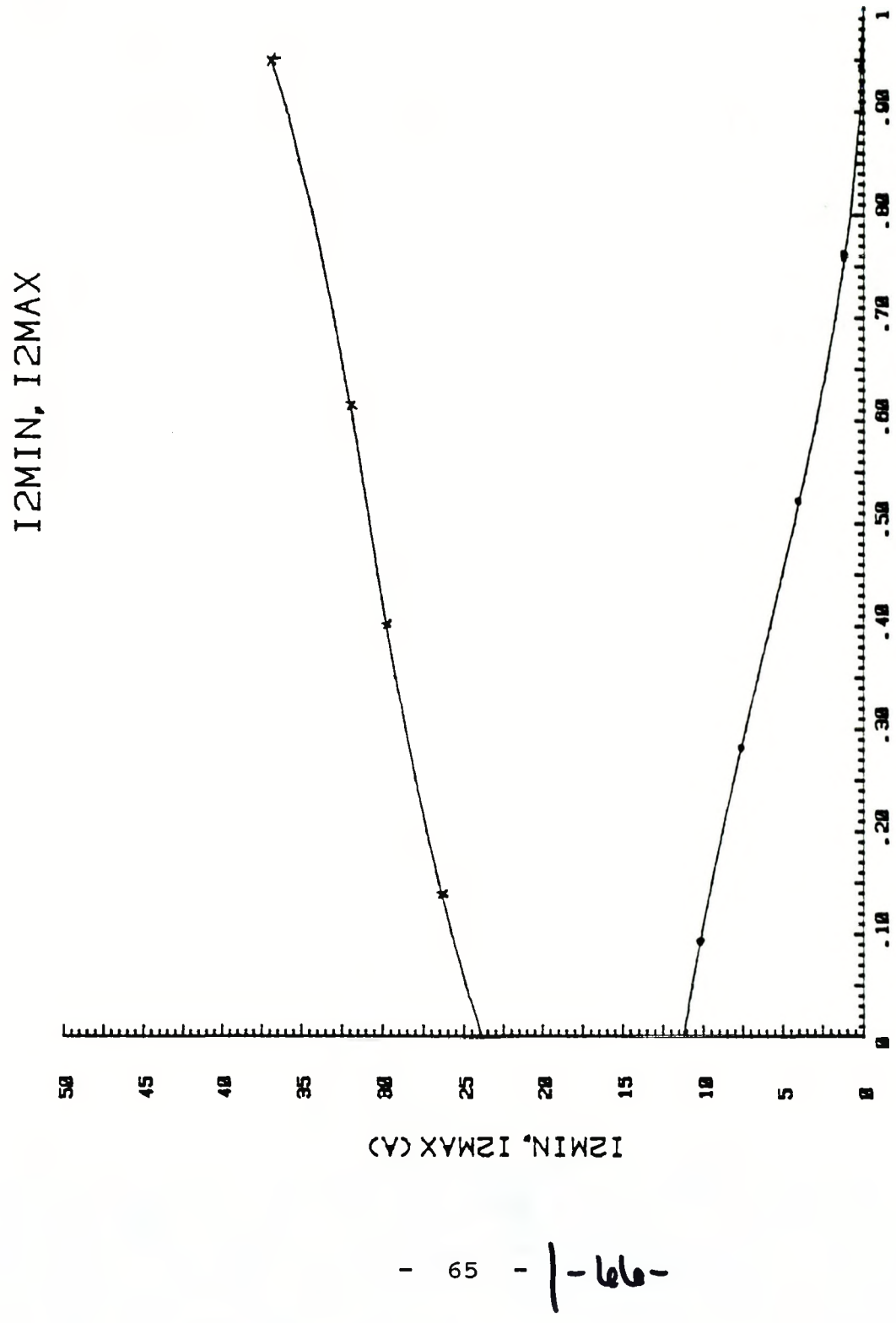

Fig.4.5 Minimum and maximum 2-pole current

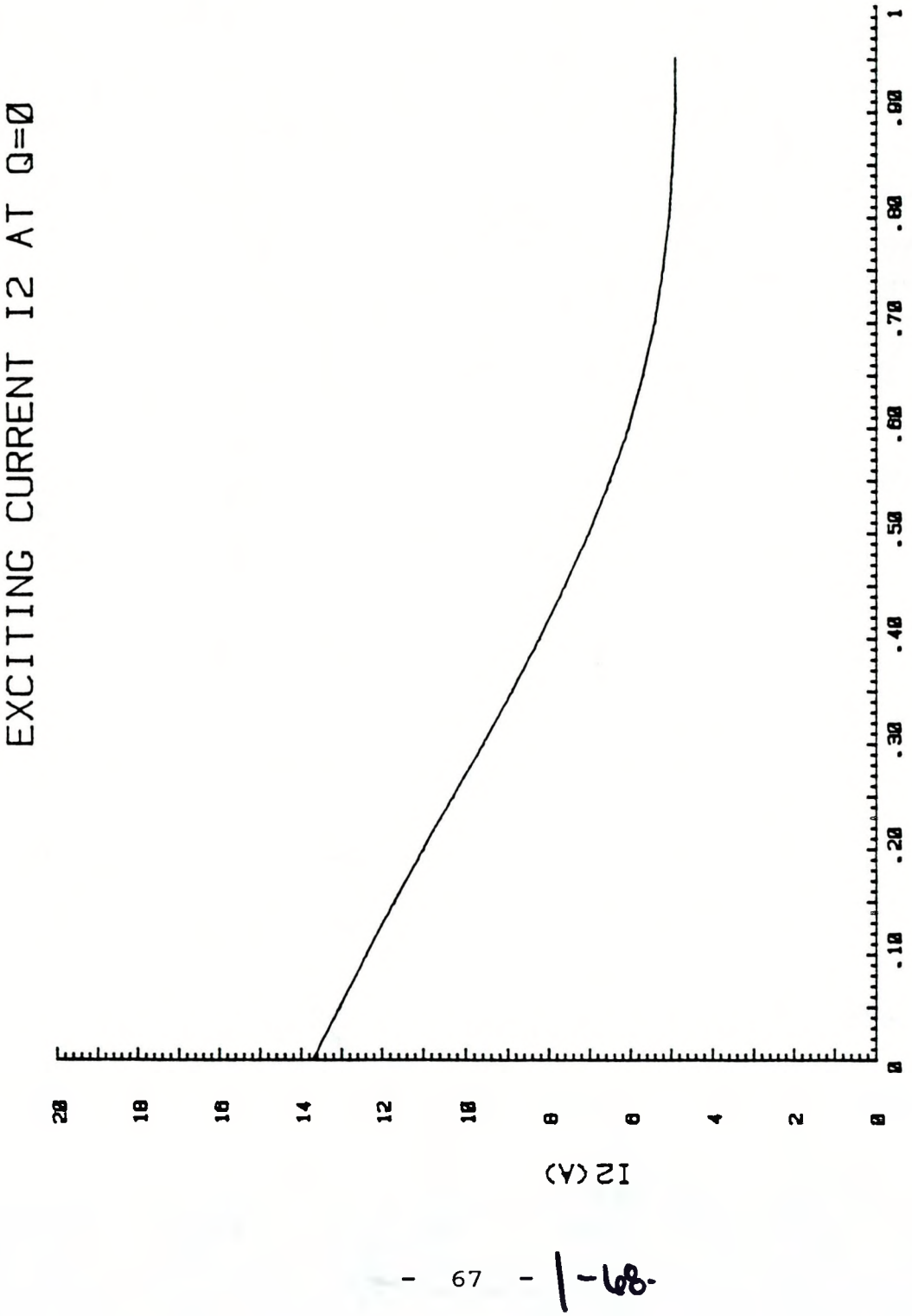

Fig.4.6 2-pole current at Q = 0

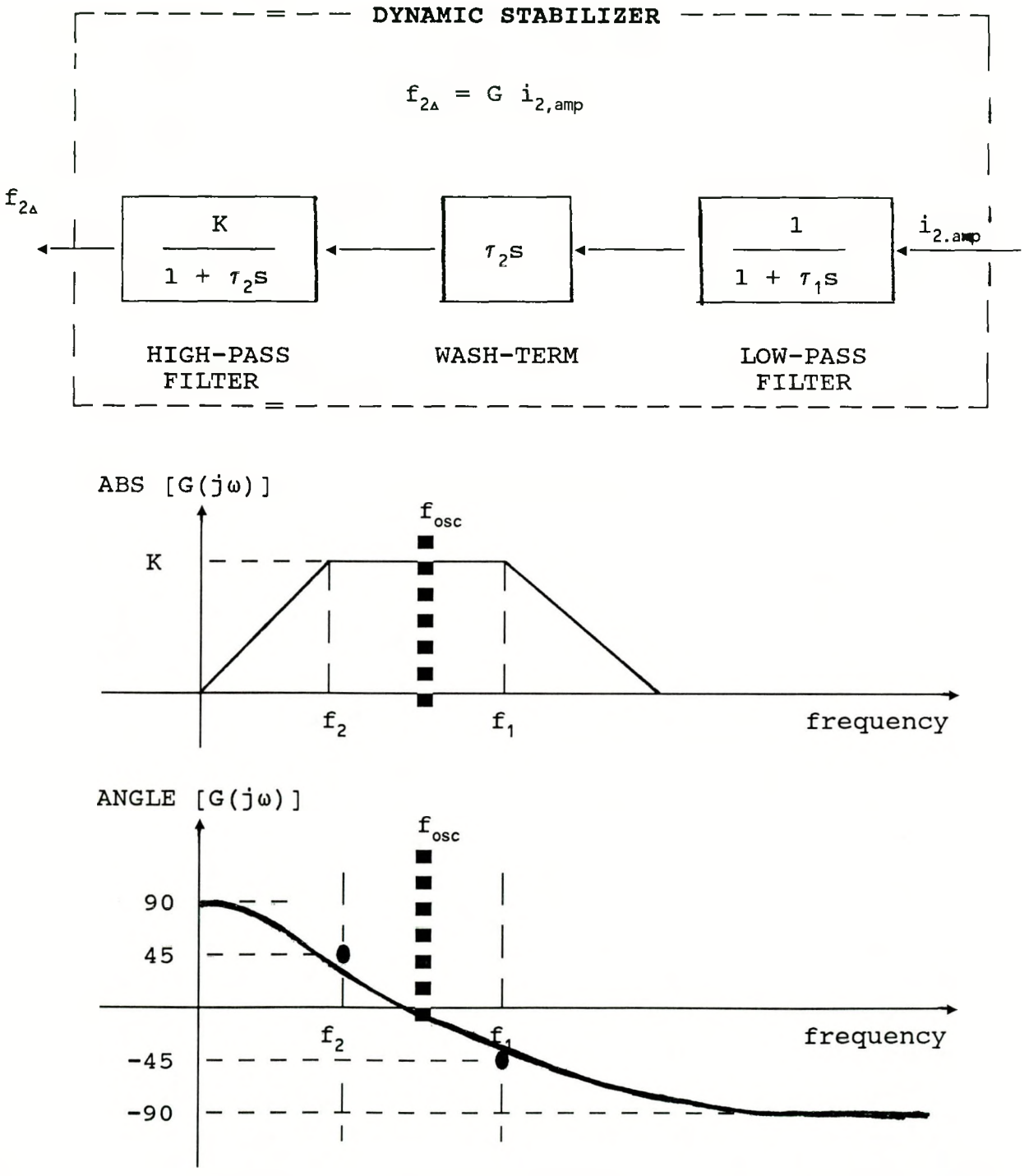

Fig. 4.7 Diagrams of Dynamic Stabilizer for current feedback.

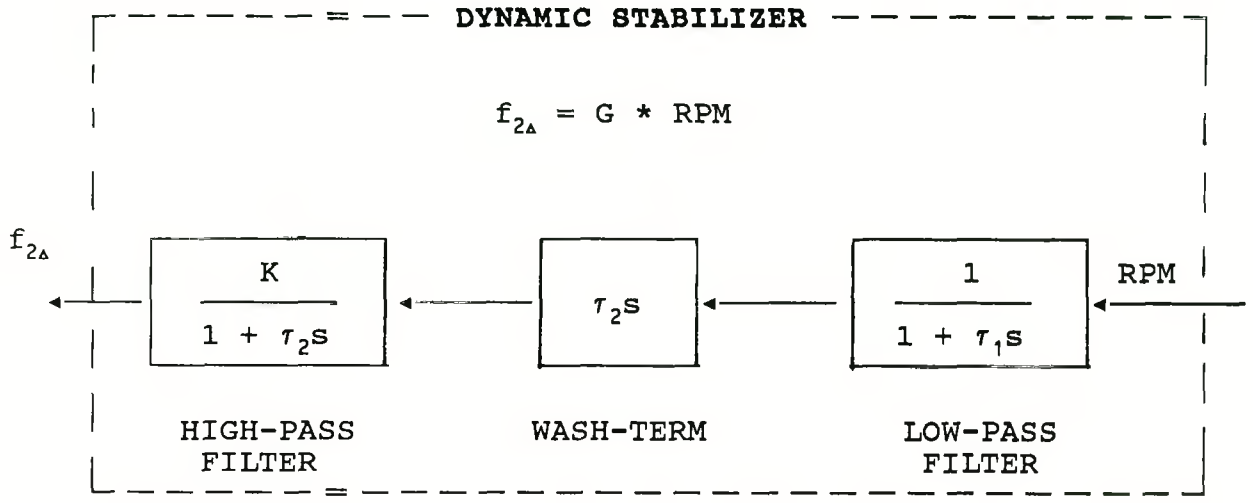

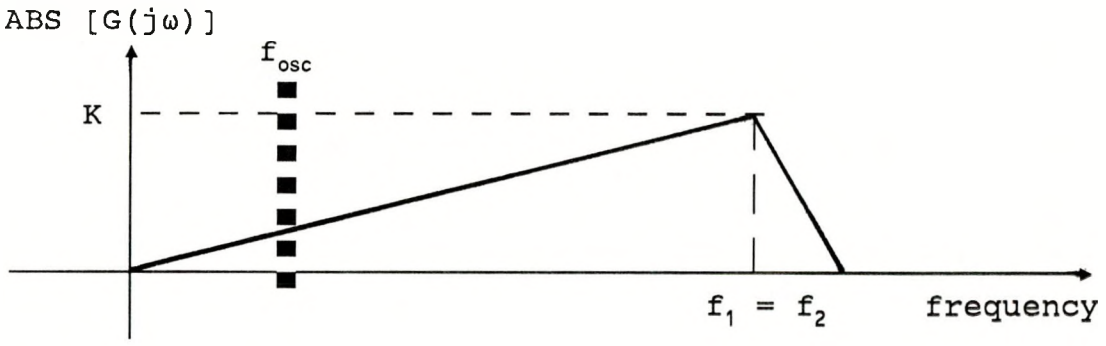

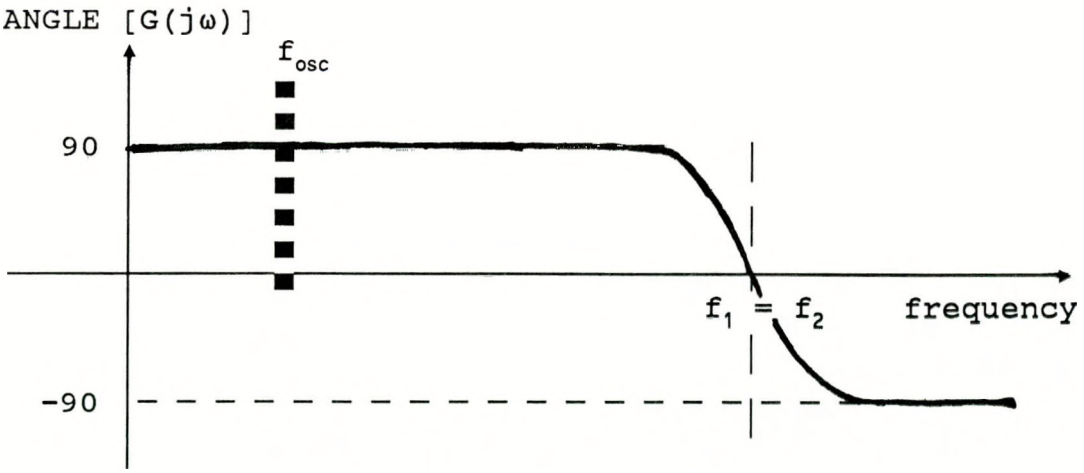

Fig. 4.8 Diagrams of Dynamic Stabilizer for RPM (shaft speed) feedback

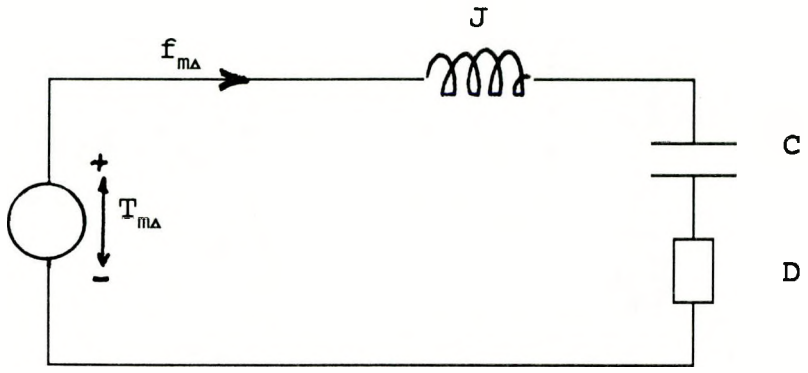

Fig. 4.9 (a) Electric Circuit Analog for the Inertial System for a conventional uncontrolled Synchronous Machine.

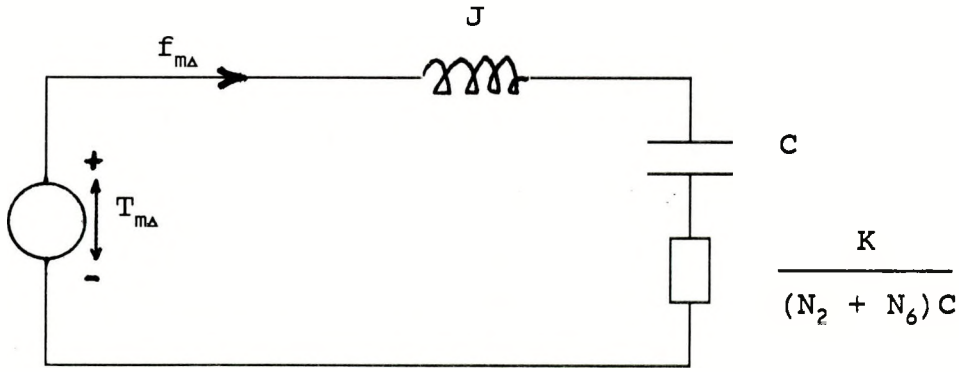

Fig. 4.9 (b) Electric Circuit Analog for the Inertial System for a controlled Brushless Doubly-Fed Machine.

5. PERFORMANCE EVALUATION

This chapter presents results of observations conducted in the energy laboratory of Oregon State University on the brushless doubly-fed machine which is connected on the 6-pole side to the utility grid and on the 2-pole side to a series-resonant converter. The converter supplies excitation power and provides a means of control for variable-speed operation. The focus is on the evaluation of the effectiveness of the stabilizer. It was mentioned before that only partial success could be established in the sense that, even though the stabilizer is capable of preventing a loss of synchronism in the unstable speed region, that bounded oscillations of this shaft-speed persist. It was also mentioned that in a later stage of the research, it became apparent that effectiveness of the stabilizer is basically hampered by the chosen winding design of the brushless doubly-fed machine. The machine was designed with common windings for the two sets of stator 3-phase systems. A modified design was pursued for a continuing research program which completely resolves the problem of the bounded oscillations. Documentation on this continuing work will not be included in this final report. Moreover, it was felt that the encountered oscillation problem renders an evaluation of the effectiveness of the voltage and reactive power controller meaningless. The design of these subcontrollers were treated in the previous chapter. Documentation of their excellent effectiveness for the modified design will likewise be postponed and presented in the final report of a continuing research contract.

5.1 STEADY-STATE STABILITY LIMITS

In Section 4.2 the stability performance of the brushless doubly-fed machine was discussed and predicted on the basis of an analysis using circle diagrams. It was explained that peculiar to the brushless doubly-fed machine is a requirement for the machine's excitation current to be held within a lower and upper limit in order to achieve stable steady-state operation. This excitation current is the current of the 2-pole stator 3-phase system

for the designed machine. The lower and upper limits are dependent on the shaft-speed and the amount of power transferred through the machine. It is remarked that for conventional synchronous machines a similar requirement only imposes a lower limit on the field current.

Fig. 5.1 shows the result of measurements of the mentioned limits of the 2-pole current and confirms the theory as discussed in Section 4.2. In the figure, the 2-pole current limits are reflected as a function of the 2-pole current frequency, rather than as a function of the shaft speed. This is since, in the synchronous mode, the shaft speed RPM is correlated to the 2-pole current frequency according to :

$$f_m = \frac{f_6 - f_2}{n_2 + n_6} \quad ; \quad RPM = 60\, f_m \tag{5.1}$$

where $n_2 = 1$ and $n_6 = 3$, which are, respectively, the pole-pair numbers of the 2-pole and 6-pole stator 3-phase systems; $f_6 = 60$, the frequency of electric utility grid to which the 6-pole system is connected and f_2 is the frequency of the 2-pole current.

The result in Fig. 5.1 is for the case that the machine is run in no-load. Similar results were observed if the machine transfers power, operating as a motor or a generator, confirming again the theoretical prediction that the region bounded by the lower and upper limit decreases with increasing shaft speed and increases with increasing torque applied to the shaft. Moreover, it was observed that the machine looses synchronism and needs to be shut down in the 2-pole current frequency range of 15 to 20 Hz, which corresponds to a shaft speed range from 675 to 600 RPM. This speed range is about the range in which as mentioned in Section 4.2, the machine is subject to a dynamic stability problem. This is the reason why, as shown in Fig. 5.1, no lower nor upper limit of the 2-pole current exist which could maintain steady-state stability.

In Fig. 5.2, the beneficial result of turning on the designed stabilizer is shown. Operation

in the mentioned unstable region at a 2-pole current frequency of 15 to 20 Hz does not require a system shut-down. The required 2-pole current satisfies the steady-state stability limits as predicted with the circle diagram analysis. However, even though system shut-down is not necessary, operation in this unstable region is not desirable because of the bounded oscillations which can be observed in the shaft speed. Therefore, effectiveness of the stabilization effort can be only qualified as partially successful. In the next section it will be shown that even an optimized stabilizer is not capable of alleviating this undesirable effect. A future report from a continuing research contract will cover the explanation and the remedy to contain this oscillation problem.

5.2 EFFECT OF STABILIZER PARAMETERS

The result of efforts to optimize the stabilizer parameters will be documented in this section. The structure of the stabilizer was discussed in the previous chapter and a block diagram of the controller presented in Fig. 4.7. Running the brushless doubly-fed machine in no-load was observed to lead to the worst oscillations in the unstable region, which was mentioned in the previous section to occur at the 2-pole frequency of about 15 Hz to 20 Hz (corresponding to a shaft speed of 675 to 600 RPM). The machine running with some load seems to benefit from additional damping by the load. Therefore, all results shown in this section are given for the worst case where the machine runs at no-load.

The machine was attempted to be run at the unstable 2-pole current frequency of 19 Hz (corresponding to 615 RPM) with the stabilizer turned off, i.e. the stabilizer output signal was not passed through to the converter's waveform synthesizer (see Fig.4.1). The resulting performance was captured in the upper plot of Fig. 5.3, where the output signal of the stabilizer $f_{2\Delta}$ is plotted. Obviously in the absence of any disturbance, $f_{2\Delta}$ is to be zero. However, the figure shows that this is far from true if the machine is attempted to be

operated in the unstable region. The oscillations in the shaft speed becomes so severe that the system needs to be shut down at the point in time indicated in the figure.

The lower plot in Fig. 5.3 shows the effectiveness of the stabilizer. The machine is again run at the unstable 2-pole current frequency of 19 Hz (corresponding to 615 RPM) and yet, the machine can be observed to be stabilized to the point that no system shut-down is required and the stabilizer output signal is kept well within bounds. This result was obtained after the application of a steepest descent method to find the best set of stabilizer parameters, i.e.,

gain K = 3.5 and the corner frequencies f_1 and f_2 respectively 3.2 Hz and 0.1 Hz.

Applying Eqn. (4.4) from Chapter 4, the time constants τ_1 and τ_2 are to be chosen equal to respectively 49 msec and 1590 msec. Note that oscillations still persist even though the machine is stabilized. No further improvement was possible with the chosen stabilizer structure. In general, the following guidelines apply in the choice of the stabilizer parameters:

(a) The lower corner frequency f_2 should be chosen considerably lower than the frequency f_{osc} of the oscillation to be "battled" (see the Bode diagram of Fig. 4.7). f_{osc} was measured to be in the order of 1.5 Hz. Increasing f_2 from the best value of 0.1 Hz to 0.15 Hz indeed causes the extent of the oscillations to grow as shown as evident from Fig. 5.4, even though system shut-down was found not to be necessary.

(b) The upper corner frequency f_1 should be chosen higher than the oscillation frequency f_{osc} such that noise on the input signal of the stabilizer is filtered out adequately.

(c) The gain K determines the sensitivity of the stabilizer. Too low of a gain causes the stabilizer to be "ignored" since the output of the stabilizer becomes negligibly small and consequently fails to transfer the information for proper compensation of the

unwanted oscillation. This is evident from the upper plot of Fig. 5.5, showing the result of lowering the gain from its best value of 3.5 to 1. An excessive value of the gain causes the stabilizer to compound the stability problem as is well known to be the effect of violating the Nyquist criterion for any feedback system. The lower plot of Fig. 5.5 shows this detrimental effect in which the gain is increased from its best value of 3.5 to 5.

5.3 SYNCHRONIZATION

This section covers the effect of the stabilizer on the synchronization process. It was mentioned in Ref. (6) that synchronization is required in order to achieve the synchronous mode of operation which indeed is the preferred mode to benefit from a higher efficiency as compared to the induction mode of operation. A number of methods were discussed and verified to be conveniently applied in practice. DC synchronization is synchronization by means of injecting the 2-pole 3-phase system of the brushless doubly-fed machine with DC current. Initially the machine is run up to near 1200 RPM as a conventional 6-pole induction machine by connecting the 6-pole 3-phase system to the 60 Hz electric grid with the 2-pole system terminals left open. Subsequently, DC current can be gradually or step-wise fed into the 2-pole system by the converter until synchronization is established, i.e the shaft speed is locked to 900 RPM. This shaft speed is the result of subjecting the 6-pole system to a 60 Hz supply while injecting the 2-pole system with DC current and can be expected from the relationship given in Eqn. (5.1) for synchronous operation.

The DC synchronization process was carried out on the designed machine and captured in the upper plot of Fig. 5.6. Following the instant of step-wise injection of the DC current into the 2-pole system, steady-state smooth operation can be observed to be established in about 6 seconds. The lower plot of Fig. 5.6 shows the result of duplicating the DC

synchronization process with the designed stabilizer turned on, demonstrating that the stabilizer clearly enhances the synchronization process. Smooth steady-state operation is achieved in about 2 seconds after step-wise injection of the DC current into the 2-pole current.

While such a reduction in synchronization time due to the stabilizer may not have any practical significance, it does indeed demonstrate the effectiveness of the stabilizer in providing extra damping to the system. This extra damping was discussed in the previous section to be sufficient for stabilizing the machine in the unstable region (525 to 675 RPM), but apparently insufficient to reduce the bounded oscillations of the shaft speed if the machine is operated in this region. However, the excellent response of the machine to the stabilizer's effort during synchronization in the stable region (at 900 RPM) strongly indicates that the stabilizer does provide a considerable amount of extra damping to the inertial system of the brushless doubly-fed machine. These seemingly contradictory results suggest that in the unstable region the machine is subject to a different phenomenon which can not be solved by a mere introduction of extra damping. Explanation and remedy to this problem will be presented in a future report from a continuing research contract.

5.4 SPEED CONTROL AND PERFORMANCE

In this section the performance of the brushless doubly-fed machine under speed control will be scrutinized. It was explained in the previous section that theoretically the shaft speed of the machine operating in the synchronous mode can be controlled without the need of a closed-loop feedback controller. The machine behaves like a conventional synchronous machine and its speed is locked to the frequencies :

f_{s6} = 60 Hz = supply frequency of the 6-pole 3-phase stator system, and

f_{s2} = supply frequency of the 2-pole 3-phase stator system.

Since the 2-pole system terminals are connected to the converter, f_{s2} is determined by the converter by which a convenient means is provided for controlling the shaft speed. The speed at which the machine runs follows from the relationship given in Eqn. (5.1). It is pointed out that the converter likewise does not require a closed-loop feedback system in order to control its output frequency. This is because the converter sustains an infinite impedance at any output frequency except at the desired frequency which can be dictated by the chosen firing schedule of the semi-conductors in the converter. Therefore, shaft speed control of the brushless doubly-fed machine can be entirely achieved in an open-loop fashion, and yet this speed can be controlled with a margin as tight as that of a conventional synchronous machine.

Fig. 5.7 shows the behavior of the shaft-speed under open-loop control of the converter. The shaft speed is changed by varying the converter frequency which in essence determines the 2-pole frequency, i.e. the frequency of the current flowing in the 2-pole stator 3-phase system. The plot results are shown for a variation in the 2-pole frequency from 5 to 10 Hz resulting in a change of the shaft speed from 825 to 750 RPM. Since the variation occurs outside the unstable region of a 2-pole frequency from 15 to 20 Hz (675 to 600 RPM), it can be observed from Fig. 5.7 that stability is not lost whether or not the stabilizer is included. The upper plot shows the result with the stabilizer turned off and the lower plot for the case that the stabilizer is turned on. It is remarked that again the additional damping effect of the stabilizer can be noticed.

In Fig. 5.8 the change of the 2-pole current frequency is carried out in the unstable region, i.e. the 2-pole frequency is changed by the converter from 15 to 19 Hz. With the stabilizer off, the upper plot shows that indeed the shaft speed does not change from 675 to 615 RPM and that synchronism is lost followed by operation of the machine in the undesirable induction mode. Effectiveness of the stabilizer is clearly indicated in the result of the lower plot for the case where the same experiment is conducted with the stabilizer turned on. Synchronism is maintained, although bounded oscillations in the shaft speed can be observed as was mentioned to persist if the machine is operated in the unstable region.

If the speed is continuously controlled to vary from 900 to 300 RPM (by varying the 2-pole frequency from 0 to 40 Hz with the converter), then the upper plot of Fig. 5.9 shows that such an attempt fails if the stabilizer is off. As the RPM enters through the unstable region from 675 to 600 RPM, synchronism is lost. The lower plot of Fig. 5.9 again demonstrates the effectiveness of the stabilizer. The unstable region is smoothly passed and as the shaft speed reenters the stable region below 600 RPM and settling with a 2-pole frequency of 40 Hz at 300 RPM, no bounded oscillations are visible.

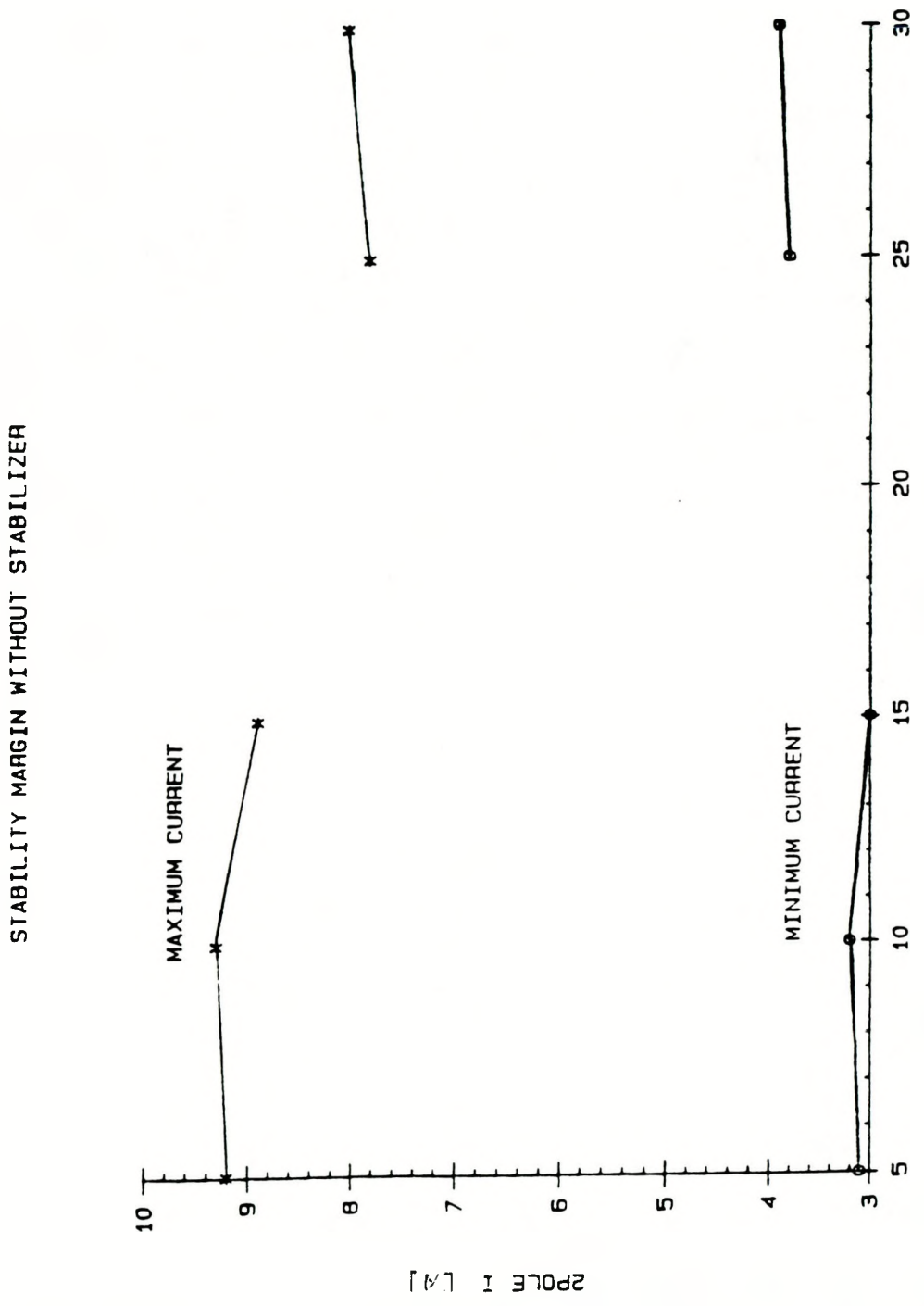

Fig 5.1 Stability Limits Without Stabilizer

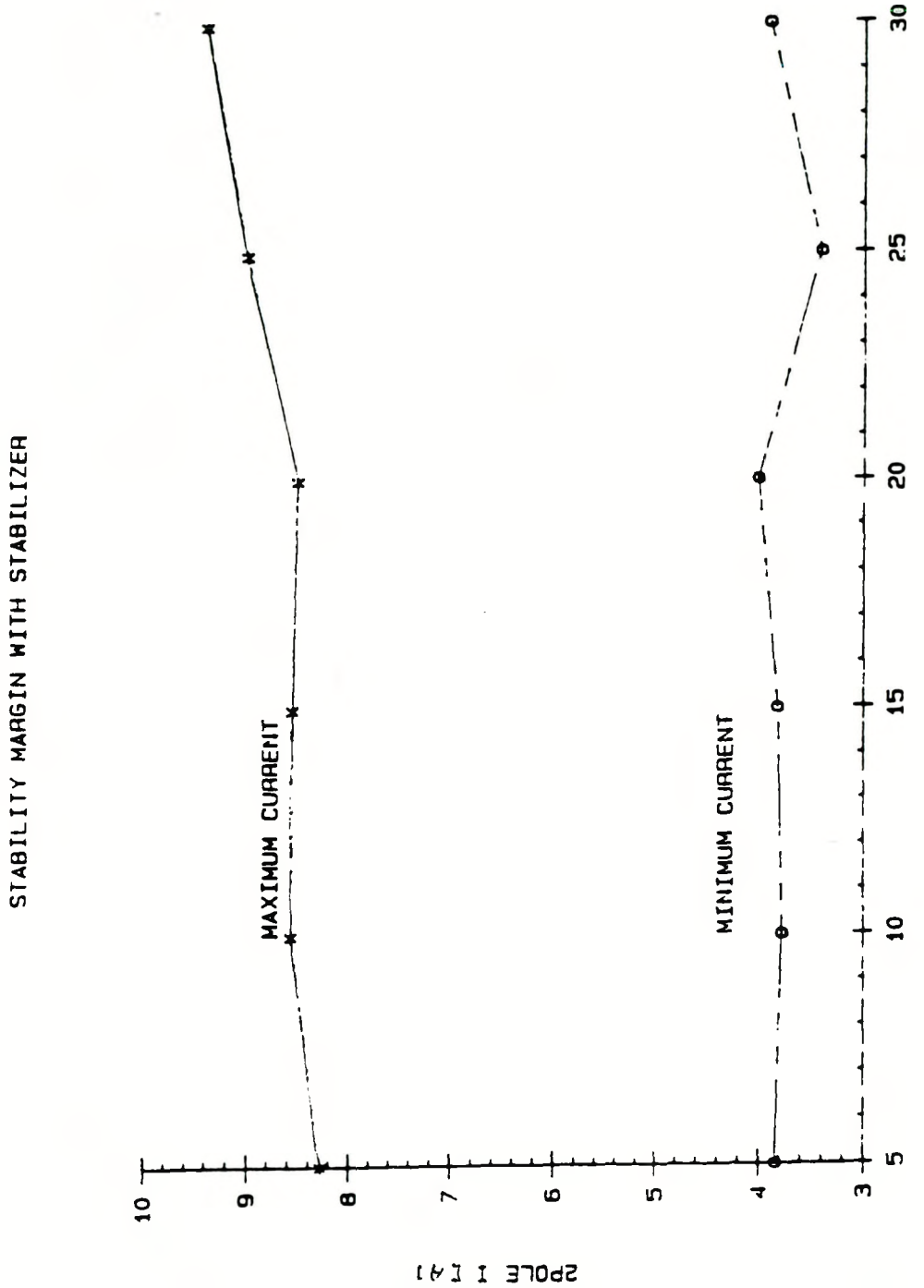

Fig. 5.2 Stability Limits With Stabilizer

Fig.5.3

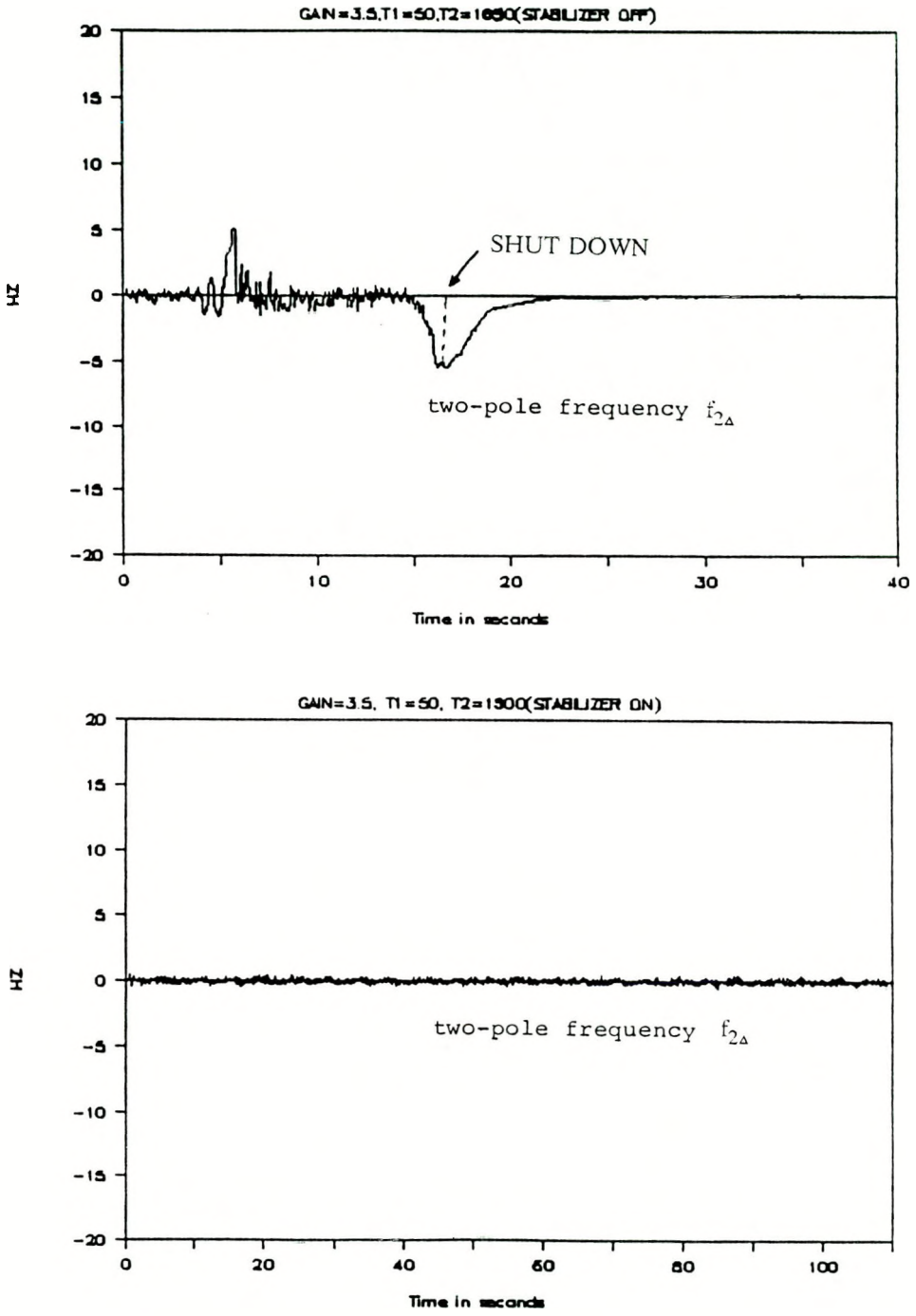

Fig. 5.3 Stabilizer Output Signal in the unstable region with the stabilizer turned off and turned on.

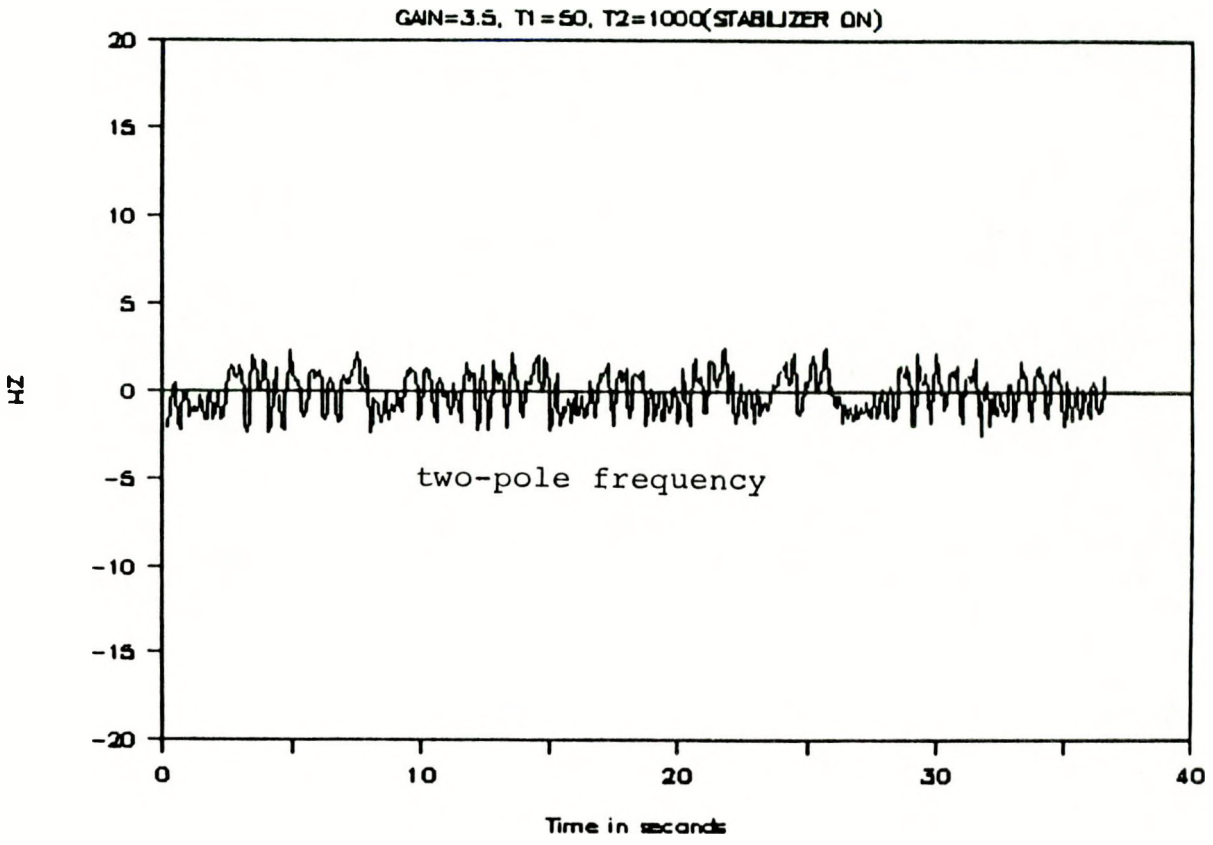

Fig.5.4 Effect of Stabilizer parameters: higher lower corner frequency

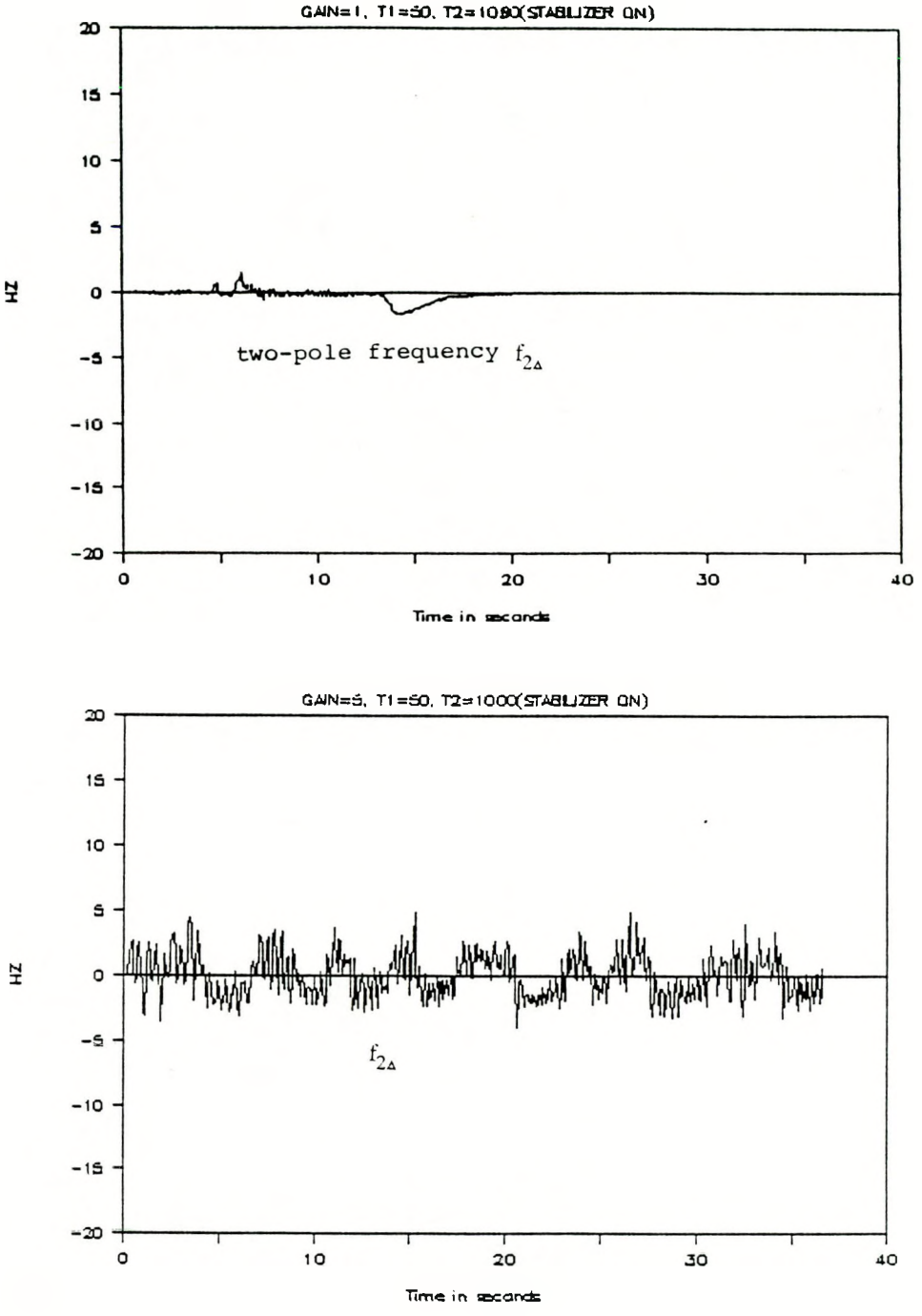

Fig. 5.5 Effect of stabilizer parameters: low and high amplification gain.

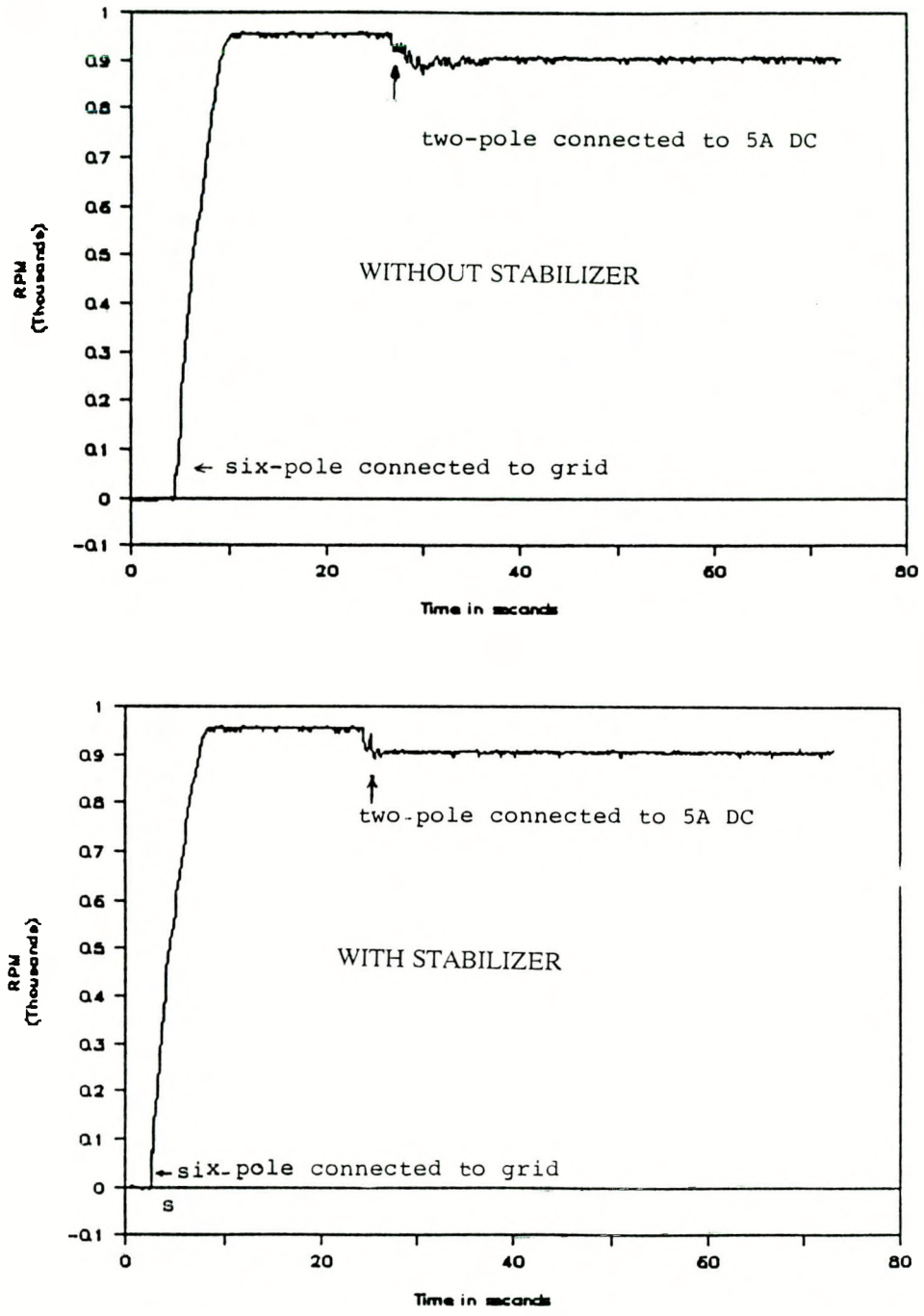

Fig. 5.6 DC Synchronization with and without the stabilizer.

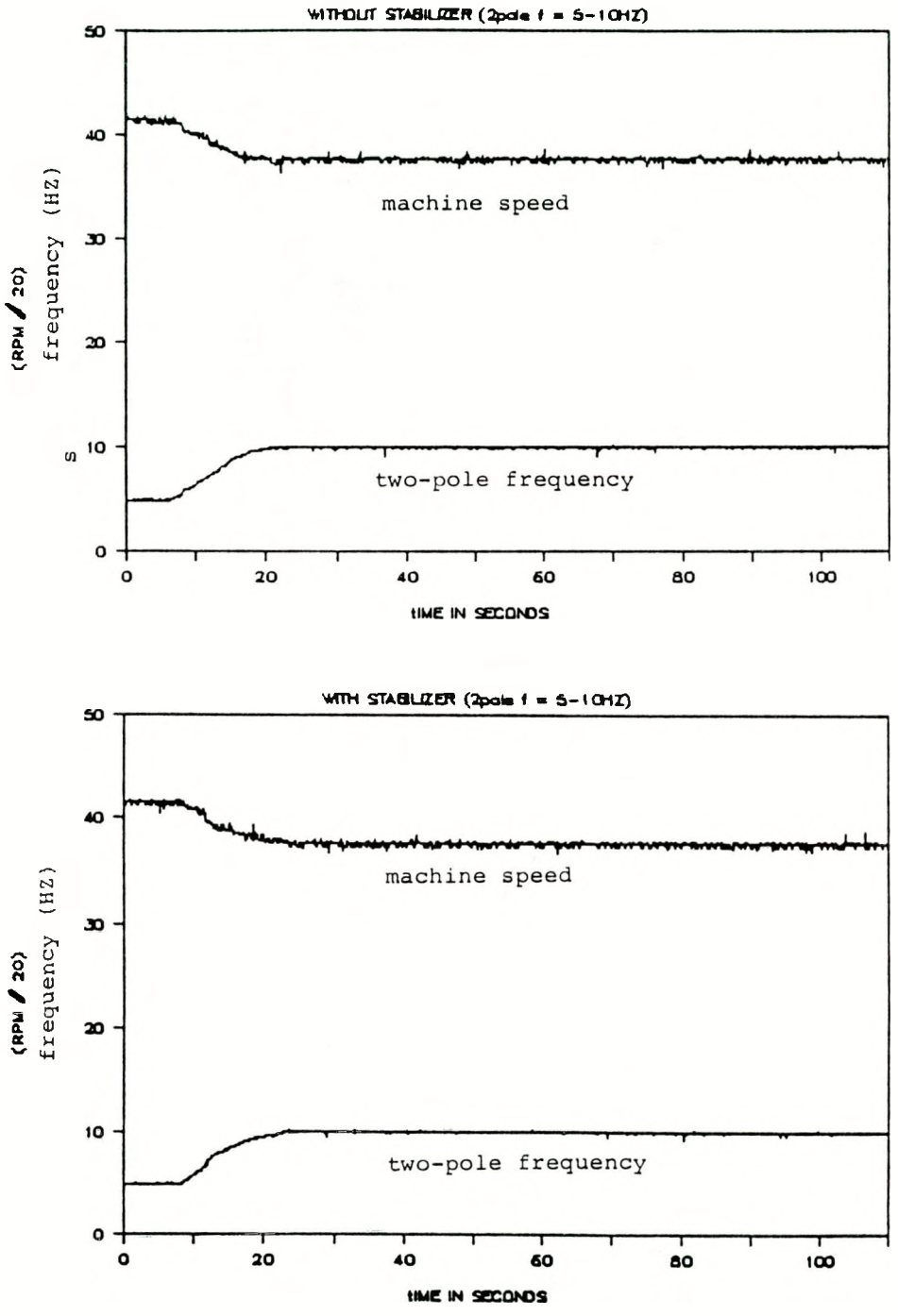

Fig. 5.7 Speed Performance in the stable region with and without the Stabilizer

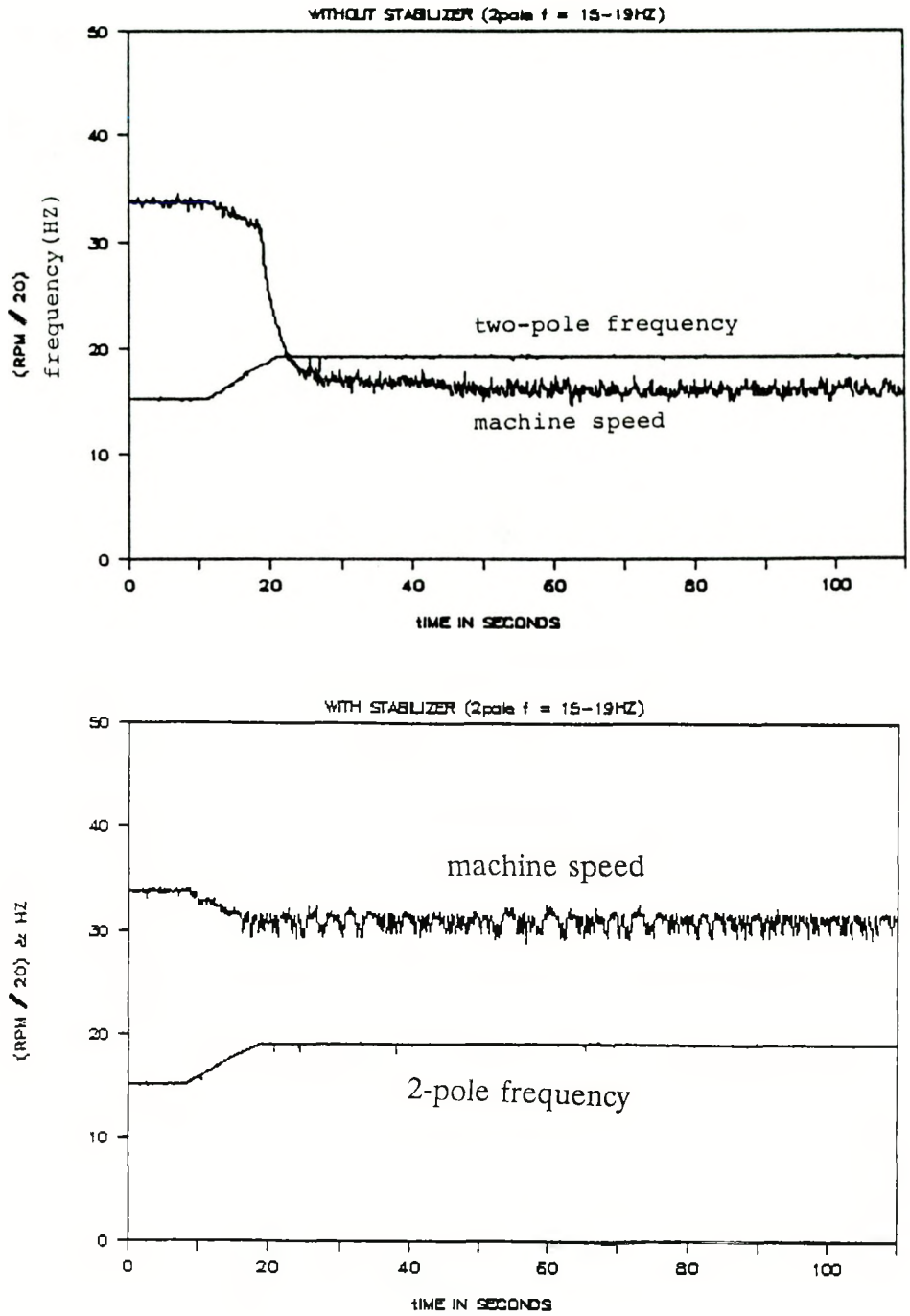

Fig. 5.8 Speed performance in the unstable region without and with the Stabilizer (after synchronization at DC).

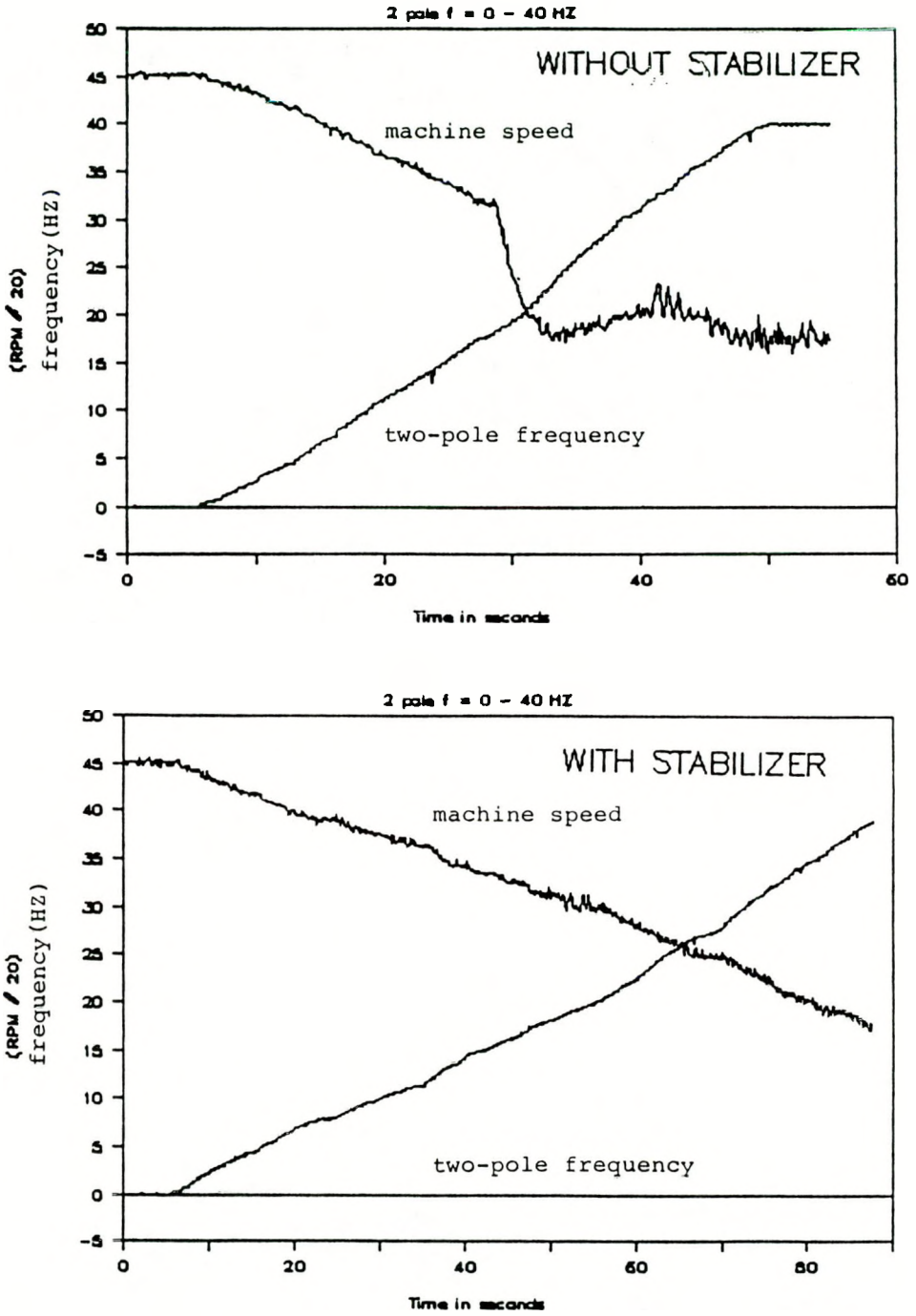

Fig. 5.9 Speed Control without and with the Stabilizer

CONCLUSIONS

The control aspects of a variable-speed generation (VSG) system using a brushless doubly-fed generator excited by a series-resonant converter have been investigated by means of an actual design of the system. The brushless doubly-fed machine comprises two sets of stator-3-phase systems which are designed with common windings. The rotor is a cage rotor resembling the low-cost and robust squirrel cage of a conventional induction machine. This VSG system is set up in the energy laboratory of the Department of Electrical and Computer Engineering at Oregon State University. The following conclusions can be drawn from these investigations.

(1) The series-resonant converter designed to achieve adequate control for variable-speed generation with the brushless doubly-fed generator was adequate in terms of required time response and regulation as well as in providing for adequate power quality. The series-resonant converter which allows for open-loop control of the shaft speed and the machine excitation has been demonstrated to be capable of establishing the required waveforms of voltage and current. The converter in essence controls the amplitude and frequency of the current flowing into the 2-pole terminals of the two sets of stator 3-phase systems. The response speed of the converter to a change in the reference signals for this amplitude and frequency was in fact so high that a delay had to be inserted in order to take into account of the slower time constants associated with the inertia of the machine.

(2) The other elements of the VSG controller, i.e. the voltage or reactive power controller, the efficiency maximizer and the stabilizer, could be designed using conventional microprocessor elements with a processing time (including data acquisition) in the order of 1 msec which is well within the time period required for sampling the variables involved with executing the control tasks.

(3) Stabilization of the conventional doubly-fed machine was demonstrated to be easily established (Ref. 3). If the machine is operated such that the requirements for steady-state stability are satisfied, then complete stability at any speed is achieved simply by operating the converter in the current-source mode. However, the brushless doubly-fed machine was observed to be dynamically unstable in a relatively small speed region (525 to 675 RPM at no-load), even if the requirements for steady-state stable operation are met. Careful observations of the dynamic stability problem within this relatively small speed region have led to the conclusion that continuous operation of the VSG system using a brushless doubly-fed machine is at such a risk, that acceptance of the machine for a VSG application should be rejected unless this dynamic stability problem can be solved.

(4) The stabilizer feedback loop which only requires current sensors to provide the 2-pole current amplitude as an input signal to the stabilizer, is elegant in that no tachometer is needed. Effectiveness of the control depends on how well the oscillations in the 2-pole current amplitude represent the shaft-speed oscillations due to the dynamic instability phenomenon. In case of a phase difference occurring between the oscillations of the 2-pole current amplitude and the shaft-speed, compensation of this phase difference is to some extent possible by adjusting the corner frequencies of the stabilizer. At the cost of including a tachometer, a different stabilizer design with the shaft-speed as input signal allows for reducing the shaft speed oscillations directly. It was shown that this method provides additional damping to the inertial system in a nondissipative manner.

(5) It was experimentally verified that the designed stabilizer was effective in that operating the VSG system in the unstable region does not require the system to be shut down. With the stabilizer turned off, shut-down is necessary in this unstable region which, during light load conditions, occur at a shaft speed of about 525 to 675 RPM. Under heavier load, this unstable region reduces in size. Moreover, it could be clearly observed that the stabilizer is capable of providing

significant extra damping to the inertia system during synchronization and during control of the shaft speed over a wide speed range.

(6) The stabilizer can only be considered partially successful in resolving the stability problem of the brushless doubly-fed machine. Even though operation in the unstable region does not cause the need for a system shut-down, it can be observed that bounded oscillations on the shaft speed persist. However, the excellent response of the machine to the stabilizer's effort in producing significant additional damping (see remark 5), strongly suggests that in the unstable region the machine is subject to a different problem which can not be contained by a mere introduction of extra damping. Explanation and remedy to this problem will be presented in a future report resulting from a new research contract.

REFERENCES

[1] H.K. Lauw: "Characteristics of the Doubly-Fed Machine in a Hydro Variable-Speed Generation System", Final Report, USDOE Bonneville Power Administration, Contract No. 79-85BP24332, June 1986.

[2] H.K. Lauw: "Variable-Speed Generation with the Series-Resonant Converter", Final Report, USDOE Bonneville Power Administration, Contract No. 79-85BP24332 Mod-1, January 1987.

[3] H.K. Lauw, L.C. Jensen, C.H. Weigand, J.W. Green, R. Sivakolundu: "Design and Implementation of the Controller for a Variable-Speed Generation System", Final Report, USDOE Bonneville Power Administration, Contract No. 79-85BP24332 Mod-2, July 1988.

[4] H.K. Lauw, J.B. Klaassens, N.G. Butler, D.B. Seely: "Variable-Speed Generation with the Series-Resonant Converter", IEEE Transactions On Energy Conversion, Vol 3, No 4, pp 755-764, December 1988.

[5] J.L. Hunt: "A New Type of Induction Motor", Proc IEE, Vol 39, pp 648-667, 1907

[6] H.K. Lauw: "Characteristics and Analysis of the Brushless Doubly-Fed Machine", Final Report, USDOE Bonneville Power Administration, Contract No. 79-85BP24332 Mod-4, June 1989.

[7] C.D. Cook and B.H. Smith: "Stability and Stabilization of Doubly-Fed Single-Frame Cascade Induction Machines.", Proc IEE, Vol 126, No 11, pp 1168-1174, 1979.

[8] J.B. Klaassens: "Series-resonant Converter System with High Internal Frequency Generating Multiphase AC-Waveform for Multikilowatt Power Levels", Power Electronic Specialist Conference, France, June 1985.

[9] EPRI Report No EP-4590: "Testing Requirements for Variable-Speed Generating Technology for Windturbine Application", 1986.

[10] J. Meisel: "Principles of Electromechanical-energy conversion", McGraw-Hill, pp 214-258, 1966.